JOURNAL OF NEUROPHYSIOLOGY
Vol. 74, No. 4, October 1995. *Printed in U.S.A.*

Influence of Eye Position on Activity in Monkey Superior Colliculus

A. J. VAN OPSTAL, K. HEPP, Y. SUZUKI, AND V. HENN
Neurology Department, University Hospital, CH 8091 Zürich; Physics Department, Eidgenössische Technische Hochschule, Hönggerberg, CH 8093 Zürich, Switzerland; and University of Nijmegen, Department of Medical Physics and Biophysics, NL-6525 EZ Nijmegen, The Netherlands

SUMMARY AND CONCLUSIONS

1. Most recording studies on the role of the monkey superior colliculus (SC) in eye movement generation have so far indicated that the code of the recruited population of cells is a fixed vector command representing the desired saccadic eye displacement vector, irrespective of the position of the eyes in the orbit. Experimental evidence from microstimulation, lesions, and neuroanatomy, however, suggests that the SC may have access to an eye position signal.

2. In this paper we have tested the hypothesis that SC activity is influenced by eye position, by recording from presaccadic burst neurons while monkeys made rapid eye movements in the light covering a large part of the oculomotor range.

3. In four alert rhesus monkeys, we obtained sufficient data from 57 SC single units. The activity of a substantial part of these cells (30/57) appeared to be significantly influenced by eye position. Although the tuning properties of these cells for saccade amplitude and direction remained invariant for changes in eye position, the peak firing rate of these units was systematically influenced by the position of the eyes in the head.

4. We have characterized this eye position dependence of a neuron's activity by a qualitative, model-independent, as well as by a quantitative model description (gain field), which takes into account both the tuning properties of the cell for eye displacement vectors and the dependence of eye position.

5. Although a majority of gain fields had their eye position sensitivity vector roughly aligned with the optimal saccade vector direction (colinear gain field, 17/30), a substantial part of the gain fields had their eye position sensitivity vectors in quite different directions, approximately homogeneously distributed with respect to the cell's ON direction.

6. We conclude that the SC has access to a signal related to the position of the eyes in the orbit. Several hypotheses on the possible functional role of this signal, in relation to the neural code of the motor map, are discussed.

INTRODUCTION

It is well established that the superior colliculus (SC) is critically involved in the generation of saccadic eye movements. Cells in its deeper layers have limited movement fields, meaning that they are recruited with an intense burst of activity just before and during saccades of particular amplitudes and directions. Both stimulation (Robinson 1972) and recording studies (Schiller and Stryker 1972) have indicated the existence of a topographically organized motor map in which neighboring cells have neighboring movement fields. A large population of cells within this map is thought to contribute to the ensuing saccade (Lee et al. 1988; McIlwain 1982; Ottes et al. 1986). Until recently it was generally held that this active population only specifies the amplitude (R) and direction (Φ) of the oncoming saccade (desired eye displacement vector) and has no relation to either the actual trajectory or velocity of the resulting eye movement. Recent evidence, however, indicates that this picture may be oversimplified. It was noted by Berthoz et al. (1986), in cat, and also by Van Opstal and Van Gisbergen (1990), in monkey, that the firing rate of some saccade-related burst neurons in the deep layers correlates with saccade velocity. Moreover, local inactivation of a small part of the motor map leads to slower, but not to smaller, saccades (Lee et al. 1988). It was also reported that electrical stimulation at near-threshold intensities leads to slower eye movements (Van Opstal et al. 1990). These findings seem to be at odds with a collicular code specifying only the desired saccadic displacement vector of the eyes. In a recent study, Waitzman et al. (1991) have proposed that so-called clipped cells in the intermediate and deep layers encode dynamic motor error, which is the instantaneous error of the eye to the target position. In their view, these cells are part of the putative local internal feedback loop that was hypothesized almost two decades ago and is thought to guide the instantaneous saccade trajectory (Robinson 1975; Van Gisbergen et al. 1981).

According to the ideas sketched above, it is assumed that the output of the motor SC represents an eye displacement signal (either static or dynamic), which is independent of eye position in the orbit. We have become interested in testing this latter assumption for two reasons.

First, in a recent paper, we have investigated the responses of collicular neurons in order to test the hypothesis that the motor SC might be involved in the neural implementation of Listing's law (the so-called Q-model) (Tweed and Vilis 1990; see Hepp et al. 1993 and Van Opstal et al. 1993, for a detailed description). We argued that, for that model to be correct, movement fields of SC neurons should represent eye movements as three-dimensional (3D) rotations, rather than as two-dimensional displacement vectors. A corollary of this argument was that a specific dependence of a cell's peak activity as a function of eye position would then be expected. In particular, the maximum firing rate should be most sensitive to variations in initial eye position perpendicular to the cell's optimal direction (Hepp et al. 1993; Van Opstal et al. 1993). Moreover, saccades evoked by electrical stimulation would have to be influenced by eye position in a well-defined way (Van Opstal et al. 1991, 1993). Although our single-unit recordings did not support the Q-model, we noted that stimulation-evoked saccade trajectories often depended rather strongly on the position of the eyes in the orbit (see, e.g., Fig. 2 in Hepp et al. 1993; and Fig. 2 in

Van Opstal et al. 1991). The observed relation with eye position, however, was not related to the encoding of Listing's law, because the effect often seemed to follow qualitatively the same direction as the evoked saccade vectors, rather than a gradient orthogonal to the evoked eye displacements.

Second, in the literature there is a substantial body of evidence provided by single-unit recordings, electrical microstimulation, collicular lesions, as well as neuroanatomy, which hint at the possibility that the deep layers of the SC may have access to an eye position signal. Only a brief account of this evidence will be presented here.

Because saccade-related cells in the deep layers have been shown to encode desired eye displacement (motor error) irrespective of the retinal target position, Mays and Sparks (1980) inferred that the activity in the deep layers must be updated by oculomotor information. This hypothesis was strongly supported by experiments in which the saccadic system needed to compensate for an unexpected disturbance in eye position caused by microstimulation of the deep layers (Schiller and Sandell 1983; Sparks and Mays 1983). Nevertheless, a direct dependence of saccade-related activity on absolute eye position has so far not been described for the monkey SC. By contrast, in cat SC, the tonic activity of some collicular cells was found to be linearly related to eye position (Peck 1986), and in a more recent study it was shown that often the visually evoked burst is systematically influenced by changes in eye position (Peck et al. 1995).

Stryker and Schiller (1975) reported that both the probability of occurrence and the size and direction of electrically evoked head movements in monkey SC depend on initial eye position. More recently, it has been reported that the trajectories of large saccadic eye movements, elicited by electrical stimulation at more caudal sites, may be influenced by the initial gaze direction (Segraves and Goldberg 1984; see also above). Electrical microstimulation in cat SC has also been shown to yield eye movements that are strongly influenced by the starting position of the eyes in the orbit (Guitton et al. 1980; McIlwain 1986, 1990; Roucoux and Crommelinck 1976).

The deficits in the precision of saccadic eye movements after reversible inactivation or after complete ablation of the SC are related to eye position (Albano and Wurtz 1982; Keating et al. 1986; Keating and Gooley 1988).

Recently, a retrogade tracer study in monkey SC demonstrated the existence of a projection to the SC from the contralateral nucleus prepositus hypoglossi (NPH) and from the medial portion of the vestibular nuclei (MVN) (Hartwich-Young et al. 1990). Interestingly, both nuclei are thought to be crucially involved in the neural integration process that constructs an eye position signal from velocity-related inputs (Cannon and Robinson 1987; Cheron et al. 1986).

The motor SC is also known to receive extensive projections from cortical areas that have been hypothesized to play a role in the processing of visual and oculomotor information. For example, the lateral intraparietal sulcus (area LIP) has topographically organized projections to the deep collicular layers (e.g., Baizer et al. 1993; Fries 1984; Lynch et al. 1985). It has recently been demonstrated that the activity of visually responsive neurons within the posterior parietal cortex (Area 7a) and movement-related activity in area LIP is modulated by eye position (e.g., Andersen et al. 1985, 1990; Zipser and Andersen 1988). Thus the peak firing rate of a parietal cell for a visual stimulus in the center of its receptive field often depends in a monotonic way on eye position. This behavior of a cell's activity has been termed a gain field, indicating the multiplicative nature of the effect (Zipser and Andersen 1988).

In the present paper we report on the influence of eye position on the activity of a number of saccade-related burst neurons in the motor SC of the macaque monkey, in a similar way as has been described for parietal cells. The possible implications of our findings for models of the collicular role in saccade generation are considered.

Part of this research has been described in a preliminary form (Van Opstal 1994).

METHODS

Subjects and surgical procedures

The activity of single cells was recorded with tungsten microelectrodes in the deep layers of the SC of four awake rhesus monkeys. The monkeys had been trained to follow a small red laser spot or a red light-emitting diode (LED) with saccadic eye movements. The monkey's head was restrained, and eye movements were recorded with a dual-search coil, allowing for 3D eye position registration. Eye movement signals as well as spike counts were sampled at a rate of 833 Hz (CED 1401, Cambridge Electronics).

Surgical procedures for head restraint, recording chamber, and dual-search coil implant are described in detail in Hess (1990), Hess et al. (1992), and Hepp et al. (1993). In short, under intubation anesthesia with N_2O/O_2, the recording chamber was implanted in stereotaxic coordinates centered at the midline over a trephine hole. The chamber was oriented perpendicularly to the horizontal stereotaxic plane. In addition, bolts were implanted to allow for stable fixation of the head during experiments. A special dual-search coil (Hess 1990) was implanted on one eye. Eye movements were recorded with the monkey's head in the center of two alternating magnetic fields (20 kHz) in spatial and phase quadrature (Skalar Instruments, Delft, The Netherlands). In the default experimental situation, the monkey's head was fixed in a position tilted nose down by 15° with respect to the horizontal stereotaxic plane.

Experimental protocol

All eye movement data and single-unit recordings, described in this paper, were collected when monkeys made eye movements in the light. As will be explained in more detail below, our analysis requires a large and uniformly distributed saccade data base for each cell, which must be obtained in a limited amount of time. Therefore, rather than letting the monkey perform in a paradigm in which it makes movements to specific targets, different experimental procedures were employed.

In the first type of experiment, we attracted the monkey's attention with pieces of food or novel gadgets, thus encouraging the animal to make saccades to the limits of the oculomotor range. In this way, typically 6–9 min of spontaneous eye movements were recorded, yielding ~1,000–2,000 saccades in all directions from a large range of different starting positions.

In the second type of experiment, aimed at extending the oculomotor range to three dimensions, monkeys were rotated in the light about five different axes. Rotations were either about an earth-vertical axis (at 0.2 Hz, ±40° amplitude), or about different earth-horizontal axes to induce nystagmus in the vertical, torsional, or vertical semicircular canal directions (with *monkeys Ce* and *Ca* at

0.5 Hz, ±30°; with *monkeys Cr* and *Yu* at 0.2 Hz, ±40°). Measurements from *monkeys Ce* and *Ca* were obtained from a vestibular setup in which the whole-body rotations were manually controlled. In later experimental sessions, with *monkeys Cr* and *Yu*, the vestibular chair was automatically controlled by computer.

In the last type of experiment (with *monkeys Cr* and *Yu* only), the monkey was put in different static roll positions (40° right- or left-ear down) to induce a static torsional counterroll of ~5°. This paradigm extended the horizontal/vertical oculomotor range even further. In agreement with earlier findings, in which we showed that the SC does not contribute a torsional signal to saccadic eye movements (Hepp et al. 1993), we observed that the induced counterroll had no influence on the discharge of the presaccadic collicular neurons.

Localization

In identifying the anatomic location of the SC, the stereotaxic coordinates of the electrode were compared with the coordinates of easily identifiable landmarks such as the trochlear nucleus, the abducens nucleus, or the paramedian pontine reticular formation.

Physiological identification was based on the response properties of single units. The initial visually evoked background activity of units in the superficial layers was usually followed by saccade-related activity of single units at deeper sites. We were able to verify the topographical arrangement of the motor map, both by recordings and by electrical microstimulation at low intensities (<50 μA).

We think our recordings were made from single SC cells, rather than from terminal arborizations of axons, because of the stability of the recordings, even during vestibular stimulation, and because units could be recorded from over considerable depth ranges.

Finally, after the conclusion of the single-unit recordings, and for a different experimental series, other landmarks like the rostral interstitial nucleus of the medial longitudinal fasciculus were inactivated with kainic acid. The animal was perfused under an overdose of pentobarbital sodium, the brain was removed, and histology was performed (*monkeys Ce, Ca,* and *Cr*). The relative coordinates of the landmarks were then checked.

Data analysis

Calibration of the dual-search coil signals was performed by a procedure described in detail in Hess et al. (1992). The result of this calibration is a parametrization of eye position as a 3D rotation vector, $\vec{r}$, where the three vectorial components are expressed in half-radians in a head-fixed Cartesian coordinate system (see, e.g., Hepp et al. 1993; Van Opstal 1993, for particular details). $\vec{r} = \vec{0}$ coincides with the so-called primary position. As has been extensively documented in earlier papers from several laboratories, including our own, Listing's law imposes a constraint on these rotation vectors for eye movements with the head at rest and upright: the torsional component of the position vector satisfies $r_x = 0$. In this way, the rotation vectors belong to a plane, which is known as Listing's plane. In all four monkeys, Listing's law was obeyed with high precision (typical torsional width of Listing's plane ~0.6° compared with an oculomotor range within this plane of 40° in all directions).

Saccades were detected by computer, applying velocity as well as acceleration criteria. Onset and offset markings were visually inspected and adjusted, if needed, by the experimenter. Saccades with marked overshoots, multiple-peaked velocity profiles, or blinks were discarded from the analysis.

All collicular cells displaying a clear burst of activity that was leading and tightly coupled to the onset of a saccadic eye movement were regarded as presaccadic burst neurons in this study. We have not attempted to systematically dissociate these cells into different functional subclasses, such as visual-movement or quasi-visual (Mays and Sparks 1980), because the required visuomotor paradigms for allowing such a dissociation were not performed. We could, however, determine whether the neural activity was clipped or unclipped, with regard to saccade termination (Waitzman et al. 1991).

The presaccadic activity of a collicular burst neuron associated with a saccade into its movement field was quantified in three different ways: *1*) the number of spikes, N_{dyn}, counted over a dynamic time window extending from 20 ms before saccade onset to 20 ms before saccade offset; *2*) mean firing rate of the cell, $\bar{F}_{dyn}$, in this dynamic window

$$\bar{F}_{dyn} = N_{dyn}/D \quad \text{(spikes/s)}$$

where D is saccade duration (in s); note that this activity measure, as opposed to N_{dyn}, can differ markedly for small and large saccades for which cells may fire the same number of spikes; and *3*) the number of spikes, N_{fix}, in a fixed time window, from 50 ms before saccade onset to 50 ms after saccade onset (e.g., Ottes et al. 1986). Mean firing rate of the cell, is then determined by

$$\bar{F}_{fix} = 10 \cdot N_{fix} \quad \text{(spikes/s)}$$

Note that, depending on whether or not a collicular unit carries a correlate in its firing behavior of saccade velocity, N_{dyn} and $\bar{F}_{fix}$ can yield different movement field descriptions for short- and long-duration saccades.

Results will be presented on the basis of the $\bar{F}_{dyn}$ activity measure. The results obtained with the other spikes-counting criteria will be considered in the DISCUSSION.

Two different methods have been followed to quantify the data. In the first method, a model-free description of eye position sensitivity on collicular responses was obtained on the basis of a selected set of saccade vectors. As will be explained below, this method is particularly well-suited when saccade vectors are homogeneously distributed across the oculomotor range. However, this condition was not always met. Therefore, in order to be insensitive to a particular distribution of saccade vectors, we have applied a second method, in which we propose a quantitative description of collicular gain fields based on the entire data set. We subsequently compared the results of this analysis with an earlier proposed model of SC movement fields without eye position sensitivity (Ottes et al. 1986).

Qualitative description of SC movement fields

To assess, in a model independent way, whether a cell was influenced by initial eye position, we first analyzed the cell's movement field qualitatively. This method furthermore enabled us to estimate initial parameters for the fitting procedures of the two model descriptions described below.

For each saccade, i, we first determined the initial eye position, (H_i, V_i), relative to the computed center of the oculomotor range. In this way, the center of the oculomotor range, rather than the primary position (see above), was taken as the origin of a head-centered coordinate frame.

From the data base of a particular cell, we then selected all saccades for which the saccade-related activity was within 75% of the absolute peak value, and denoted the obtained amplitude and direction ranges of these near-optimal saccade vectors as the presumed center of the cell's movement field.

Subsequently, a first-order estimate of the effect on a cell's activity due to changes in eye position was obtained for all these near-optimal saccade vectors, by fitting a best plane (in the least-squares sense) through the data according to

$$F_i = f_0 + f_H \cdot H_i + f_V \cdot V_i \qquad (1)$$

with f_0 (spikes/s) and (f_H, f_V) in spikes/s/deg. Because collicular neurons are tuned for specific saccade vectors, it should be noted that systematic differences in the distribution of these vectors across the oculomotor range may be wrongly interpreted as an eye position effect. Therefore, to address this potential problem, additional statistical tests were performed on these data by assessing the properties of the saccade vectors and cell activity within various sectors of the oculomotor range (see below, *Statistical evaluation*).

We have also explored a different method for yielding a more robust description of an eye position influence, which is based on the entire data base rather than on a selected subset of saccades. To that means we fitted the cell's movement field according to the model descriptions presented below.

Model description of SC movement fields

We quantified collicular movement fields in two different ways. In the first description we took into account the possibility that the activity of the cell might be a function of both the coordinates of the saccade vector as well as eye position. This analysis was called the collicular *gain field* description. In the second description we assumed that the cell's activity only depended on the coordinates of the saccade vector. This was termed the classical *movement field* analysis.

To determine a cell's gain field, we applied a model fit to the data by applying the following procedure.

1. For each saccade vector, i, with polar coordinates (R_i, Φ_i), and initial eye position relative to the center of the oculomotor range, $(H_i, V_i$; see above), we took the cell's activity, F_i. We then applied the χ^2-minimalization procedure of Levenberg-Marquardt (Press et al. 1992), to fit the cell's responses for the complete set of N saccadic eye movements in the light with the following planar gain field activity function

$$F_i = (a \cdot H_i + b \cdot V_i + F_0) \cdot \exp - \frac{(u_i - u_0)^2 + (v_i - v_0)^2}{2\sigma_p^2} \quad (2)$$

In this equation, u_i and v_i are the anatomic collicular coordinates, which are determined by applying the complex logarithmic mapping function of the SC motor map to each saccade vector $(R_i, \Phi_i$; see APPENDIX for additional details) (see also Ottes et al. 1986; Van Opstal et al. 1990). The six free parameters for the gain field fit are therefore the eye position modulation vector (or the *gain field gradient vector*) $\vec{a} = (a, b)$ (in spikes/s/deg), the peak activity of the cell for saccades from the center of the oculomotor range, F_0 (in spikes/s), the optimal saccade vector expressed in collicular coordinates, $(u_0, v_0$; both in mm), and the tuning width of the cell to motor error, measured as the range of collicular space in the motor map, σ_p (in mm).

2. To test whether the classical movement field function, i.e., one without eye position modulation, could describe the data equally well, we also fitted the same data set with a Gaussian tuning function to motor error, as previously proposed in the literature (Ottes et al. 1986; Van Opstal et al. 1990).

$$F_i = F_0 \cdot \exp - \frac{(u_i - u_0)^2 + (v_i - v_0)^2}{2\sigma_p^2} \quad (3)$$

Statistical evaluation

PITFALLS. We are aware that certain hidden relationships may obscure, or even cause, an apparent eye position–related effect on the activity of SC cells. First, because collicular units are tuned for a limited range of amplitudes and directions, a systematic bias in the distribution of saccade vectors as a function of eye position may cause unwanted changes in the qualitatively obtained parameters of *Eq. 1* and may thus be erroneously attributed to an eye position effect proper. Two independent tests were applied to investigate this problem.

1. To check whether the distribution of saccades into the center of the movement field (defined above) differed for various eye position sectors, we computed for these saccades the two-dimensional, two-sampled Kolmogorov-Smirnov (d) statistic (Press et al. 1992), pair-wise among different eye position sectors evenly divided over the oculomotor range, and oriented parallel to the fitted gradient vector (f_H, f_V) of the gain field (see also RESULTS, *Eq. 5*, for further details on this latter procedure). When this statistic is insignificant, e.g., $[P(d) > 0.2]$, the underlying saccade distributions are statistically indistinguishable at the obtained probability level. Thus, in those cases, an eye position effect on the cell's activity cannot be readily explained by differences in the distribution of the saccade vectors across eye position sectors.

2. Sometimes, however, the d statistic on saccade distributions proved to be significant, so that differences in saccade vectors could potentially underly the qualitatively observed eye position effect of *Eq. 1*. Therefore we had to rely on a different criterion in order to decide whether the gain field could be due to this artifact, or whether it was nevertheless likely to be real. To that means, the prediction of the cell's activity for the actually measured saccades, according to the fit results of the classical movement field (*Eq. 3*), which assumes no eye position modulation, was compared for different regions of eye positions across the oculomotor range. If a systematic bias in the saccade vector distributions would underly the observed gain field, this prediction should then also display a clear, but false, effect for these different eye position sectors. Although such a relation is still compatible with a real gain field, cells for which such a relation did indeed emerge were not included in our population of identified gain field cells.

A second hidden variable, which could have an influence on the results, resides in the possibility of a relation between saccade velocity and the activity of certain SC cells (see INTRODUCTION). For example, suppose that centripetal saccades would be associated with higher firing rates than centrifugal saccades due to a systematic higher velocity. Because we are interested in a pure eye position contribution to a cell's activity, it might prove difficult to establish such a relation if these kinematic effects exist. Therefore, to test for a systematic relation between eye position and eye velocity for saccades directed into the center of the movement field, we subjected these movements to a robust linear regression analysis, according to the following equation

$$\bar{V} \equiv \frac{R}{D} = \alpha + \beta \cdot R \quad (4)$$

where $\bar{V}$ is mean eye velocity (in deg/s), D is saccade duration (in s), and R is saccade amplitude (in deg). The parameters α (in deg/s) and β (in s^{-1}) were found by minimizing absolute deviation, rather than least-squares error (Press et al. 1992). In this way, the regression coefficients, which are based on relatively few data points, are less sensitive to outlying data points.

CONFIDENCE INTERVALS OF GAIN FIELD PARAMETERS. To test whether the eye position modulation vector, $\vec{a}$, found by the fitting procedure of *Eq. 2*, differed significantly from zero, we determined the confidence limits of (a, b) by applying the bootstrap method (Efron and Tibshirani 1991; Manly 1991; Press et al. 1992). In short, the fit on the data was repeated 250 times on data sets of equal length (N data samples of $[H_i, V_i, u_i, v_i, F_i]$), which were generated by drawing at random with replacement (with a uniform random generator) from the original data set of N points. In this way, each realization of a new data set yielded different parameter estimates, because the data distribution was different each time. From the 250 parameter estimates, means and standard deviations were obtained. These values were taken as the most reliable estimates for the parameters and their 68% confidence

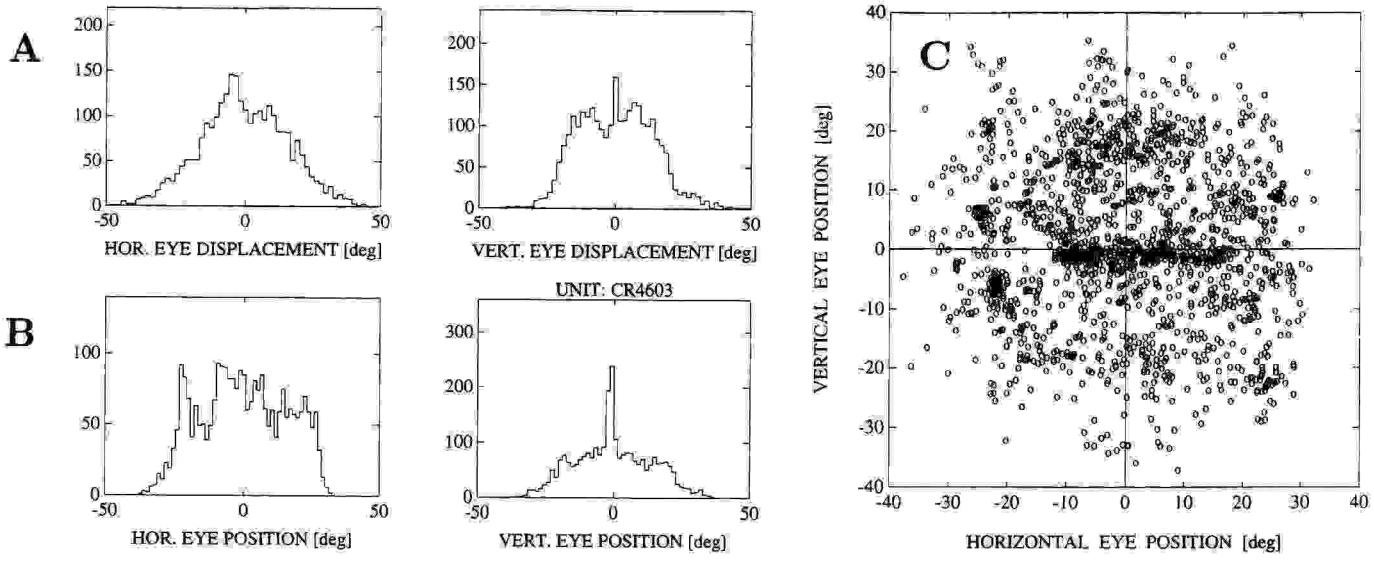

FIG. 1. Statistical properties of eye movements while recording from *cell cr4603*. *A*: distribution of horizontal (*left*) and vertical (*right*) saccade components. Note that both histograms are approximately symmetrical and peak around 0°. Means: $\mu_{\Delta H} = 0.0$, and $\mu_{\Delta V} = 0.3°$. Widths: $\sigma_{\Delta H} = 14.6$, and $\sigma_{\Delta V} = 12.9°$. Total number of saccades: $N = 2{,}735$. *B*: histograms of horizontal (*left*) and vertical (*right*) initial eye positions for the same saccades as in *A*, relative to the center of the oculomotor range. *C*: distribution of initial eye positions, re $\vec{C} = (0, 0)$, for the subset of saccades from *A* with amplitudes between 10 and 25° (see text). Note homogeneous oculomotor range with a radius of ~30°. Number of selected saccades: $N = 1{,}531$.

level, respectively. A gain field, based on this analysis, was considered significant when at least one of the two parameters (a, b) had a mean value different from zero by at least two standard deviations (95% acceptance level).

CORRELATION ANALYSIS. The parameters yielded by fitting *Eqs. 2* and *3* to the data were also used to predict the cell's activity for each measured set of eye movement coordinates $[H_i, V_i, u_i, v_i]$. In this way, linear correlation coefficients were obtained between measured and predicted firing rates for each of the two models, r_{GN} and r_{CL}, respectively. Under the assumption of normally distributed measurements (see, e.g., Fig. 1*A*) and additive Gaussian noise in the cell's activity, a standard statistical test was performed on the significance of the difference between the two correlation coefficients (Press et al. 1992). Because the number of data points was usually very high (N typically >2,000), differences in the correlation coefficients as low as 0.01 could reach a significance level as low as 0.001.

SIGNIFICANCE OF GAIN FIELDS. As will be made clear near the end of RESULTS, we have applied several statistical criteria that had to be fulfilled simultaneously in order to accept the significance of a cell's gain field. To clarify these criteria, the full procedure of our analysis will first be shown for a typical neuron.

RESULTS

General remarks

In this paper we report on a total of 57 presaccadic burst neurons from the intermediate and deep layers, obtained from 7 colliculi in 4 monkeys. From these units, we obtained sufficient data in order to allow for a full statistical analysis.

In what follows, we will first show, in subsequent figures, the various steps of our qualitative and quantitative analysis for one of these cells (*cr4603*) that has been identified for having a significant modulation of its activity by eye position. The neuron has a modest gain field but is selected because it is illustrative for most of the problems described in METHODS.

Statistics of saccades and initial eye position

The two panels of Fig. 1*A* show the distributions of horizontal (*left*) and vertical (*right*) saccade vector components of *monkey Cr* as they were collected during the recording of *cell cr4603*, while the monkey was making spontaneous eye movements in the light (number of saccades: $N = 2{,}735$). Note that both histograms are approximately normally distributed with average values close to 0.0° and comparable standard deviations of 14.6 and 12.9°, respectively. These histograms indicate that there is no obvious bias in the direction of the saccade displacement vectors, which would show as a marked skewing of these distributions. In addition, the majority of the saccades have amplitudes up to ~20°, which agrees well with earlier reports (Bahill et al. 1975). The two panels of Fig. 1*B* show the distributions of the initial eye position components re to the center of the oculomotor range (see METHODS) for the same saccades as in the *top two panels*. Note that the position histograms have approximately the same widths as the saccade distributions, although the shape of the horizontal position histogram is more uniform. The distributions for this particular recording are representative for all four monkeys.

We observed that the oculomotor range (illustrated in Fig. 1*B*), as well as its center relative to primary position (see METHODS) remained quite stable over time. The center of the oculomotor range, $\vec{C}$, was found to be located within 10° from primary position in all four monkeys (e.g., mean position of $\vec{C}$ re primary position in *monkey Cr*, averaged over 16 experimental days: $[C_H, C_V] = [-3.3, -4.1]$ deg. Variance around the mean: [2.8, 3.4] deg).

A qualitative plot of the tuning curve for this cell as a function of saccade amplitude indicated that the maximal activity was reached for saccades with selected amplitudes between 16.0 and 20.0° at an optimal direction of about $\Phi \approx 60°$ (see below, where these numbers are specified by a more

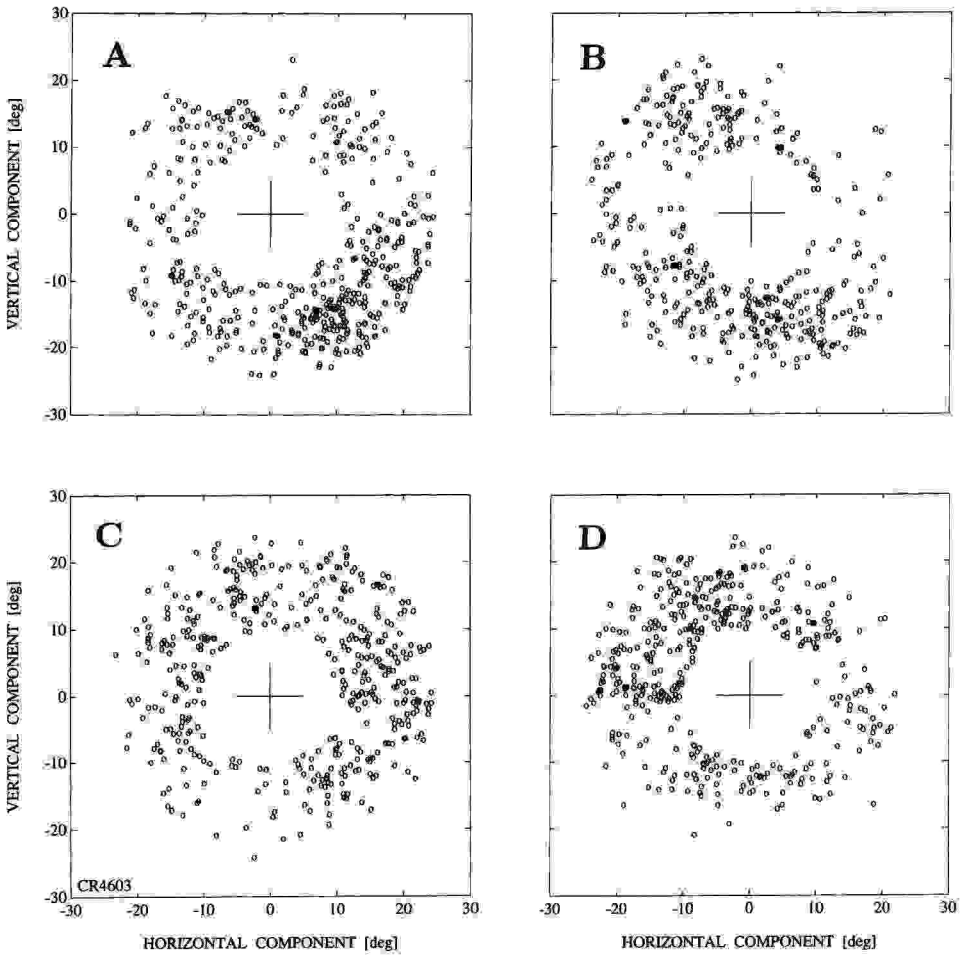

FIG. 2. Distribution of selected saccade vectors of Fig. 1*C* in each of the 4 eye position quadrants. Note approximately equal number of saccades in each sector: Right and Up: $N_{R+U} = 338$; Left and Up: $N_{L+U} = 411$; Right and Down: $N_{R+D} = 375$; Left and Down: $N_{L+D} = 407$.

precise quantitative analysis). The peak reduced to 75% of its maximum value for amplitudes down to ~10.0° and up to ~25.0°. We therefore selected, from the complete data base of the saccades in Fig. 1*A*, all saccades having amplitudes between 10.0 and 25.0°.

Figure 1*C* shows all initial eye positions for these selected saccades ($N = 1{,}531$), plotted relative to the center of the oculomotor range. The two cross lines divide the oculomotor range in four equal quadrants relative to $C = (0, 0)$. In the illustrations that follow (Figs. 2, 3, 6, and 7), data are presented in corresponding panels for each of these four eye position quadrants.

Approximately equal numbers of saccades belong to the four quadrants, which is shown in Fig. 2. In this plot, the Cartesian coordinates of the selected saccade vectors ($R \in [10, 25]$ deg) are plotted within each of the four eye position sectors. A qualitative inspection of this figure suggests that there is no strong bias for specific saccade directions. Specifically, the direction bins for saccades into the cell's movement field (around $\Phi \approx 60°$, i.e., rightward and upward), contain approximately equal numbers of saccades in three of the four quadrants (exception is quadrant 1 in Fig. 2*B*).

Figure 3 shows, for the identical set of selected saccades as shown in Figs. 1*C* and 2, the averaged directional tuning curves for this cell in the four different eye position quadrants. Each point is computed by taking the average activity (based on the $\bar{F}_{dyn}$ criterion, see METHODS) of all saccades belonging to a directional sector within 20° of the given bin. Bins are spaced at 10° intervals, so that each average value is computed by overlapping saccade populations. Upward directed lines on each data point correspond to one standard deviation for the corresponding bin. Several points are worth mentioning. First, the large standard deviations can be attributed to at least two causes.

1. The cell is tuned for both direction and amplitude. Because saccades, for which a given average is computed, are distributed over the entire two-dimensional bin of $R \in [10.0, 25.0]$ deg and $\Phi \in [\Phi_{bin} \pm 20]$ deg, a substantial range of firing rates may be expected.

2. Intrinsic variability of collicular activity, even for identical saccade vectors, may be considerable (~40% of peak firing rate) (see, e.g., Ottes et al. 1986; Stanford and Sparks 1994; Van Opstal et al. 1990). Second, the tuning curves reach their peaks in approximately the same optimal direction bin ($\Phi = 60°$), irrespective of initial eye position. Third, there appears to be a tendency for the cell to fire at a higher rate in the lower half of the oculomotor range, when compared with the two upper quadrants. Such a gradual trend persists, even if the oculomotor range is divided in a square of 16 sectors (see below, Fig. 4*B*).

In Fig. 4*A* the saccades directed into the center of the cell's movement field ($N = 132$; defined in METHODS) are

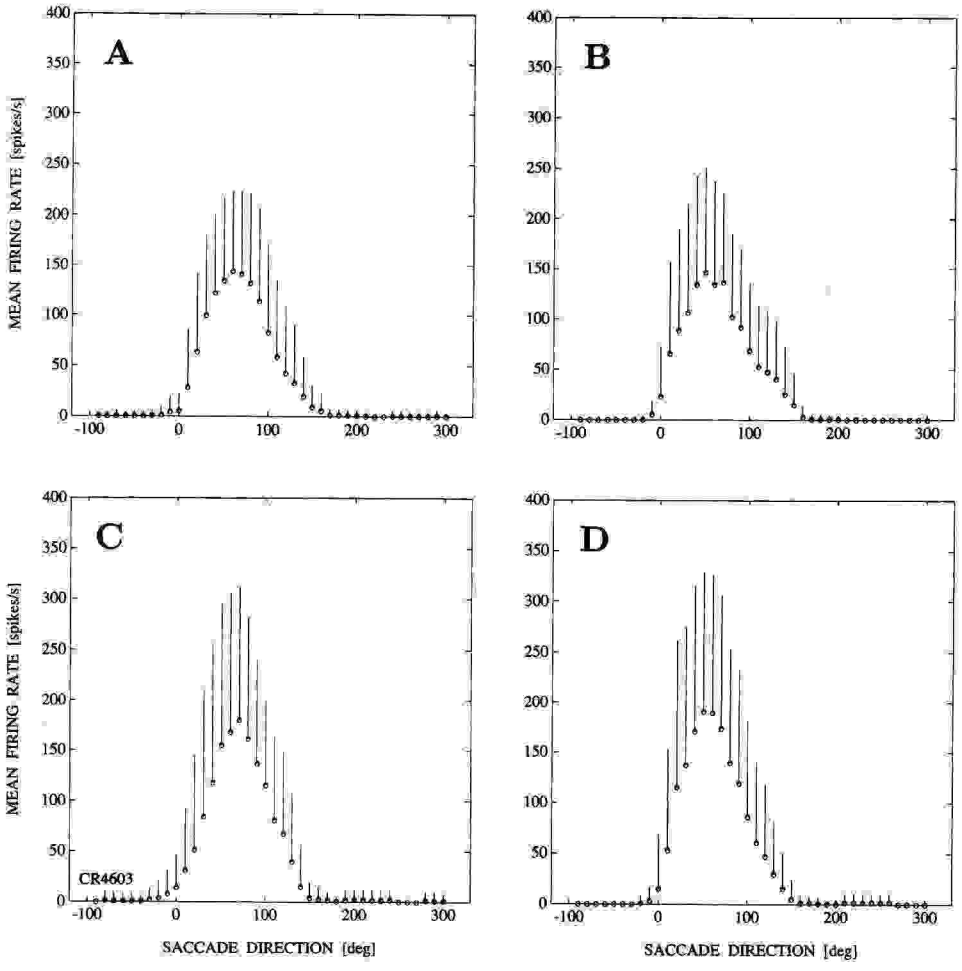

FIG. 3. *A–D*: tuning curves of *cell cr4603* as a function of saccade direction for each of the 4 eye position sectors. Data points are at 10° direction intervals. A data point of a given direction bin, Φ_{bin}, is computed from the average firing rates, F_{dyn}, for all saccades with amplitudes between $\Delta R \in [10, 25]$ deg (see Figs. 1*C* and 2), and directions in the $\Delta\Phi_{bin} \in [\Phi_{bin} - 20, \Phi_{bin} + 20]$ deg interval. Note that direction bins thus overlap. Upward directed lines correspond to 1 standard deviation around the mean (in spikes/s). Note the systematically higher peaks of the tuning curves in the lower half of the oculomotor range (*C* and *D*), when compared with the 2 upper quadrants (*A* and *B*).

plotted as straight lines between saccade onset (+) and offset (○) in a coordinate system relative to the computed center of the oculomotor range (see Fig. 1*C*).

Subsequently, the oculomotor range was divided in a 4 × 4 matrix (each sector 20° wide, and 25% overlap with neighboring sectors), and mean firing rate of the cell was computed for each of these 16 eye position bins. Figure 4*B* provides a mesh plot of these peak firing rates, in which a clear and gradual gradient of the cell's activity with eye position can be discerned. The activity is substantially higher for downward eye positions, when compared with upward initial positions. Multiple regression of the measured mean firing rates for the population of 132 optimal saccade vectors of Fig. 4*A* (*Eq. 1*) indeed resulted in an optimal plane with a gradient in the downward direction: $(f_H, f_V) = (-1.2, -4.1)$ spikes/s/deg (f_0 = 160 spikes/s).

To show that the selected saccade vectors are homogeneously distributed along the gain field gradient direction, we have computed the two-dimensional Kolmogorov-Smirnov statistic (see METHODS) for two eye position sectors equally spaced along (f_H, f_V), by applying *Eq. 5* to these data. Figure 4*C* shows the distribution of the saccade vectors [plotted relative to the estimated center of the movement field, $(R, \Phi) = (16.5, 60)$ deg], for each of these two halves (open circles: upward eye positions, N = 73; asterisks: saccades belonging to the downward sector of eye position, N = 59). The probability of the d-statistic is found to be 0.33, which indicates that it is highly likely that the two saccade vector populations have been drawn from the same probability distribution. The average firing rates in these two sectors is, however, significantly different (Student's t-test = −2.5; $P(t) < 0.01$). Similar results are obtained when eye positions are divided over three equal sectors along the fitted gradient direction (not shown).

To check whether perhaps the observed influence of eye position on the cell's firing rate could be attributed to a systematic change in saccade kinematics, mean eye velocity of saccades within a narrow amplitude bin (i.e., within 10% of the estimated optimum amplitude, which in the case of *cell cr4603* was 16.5°, see below) was plotted as a function of saccade direction in the same format as Fig. 3 and inspected for systematic trends. In all four eye position quadrants, the mean eye velocity of the saccades within the $\Phi = 60 \pm 20°$ bin had similar values (414 ± 16°/s averaged over the 4 quadrants; not shown). Thus we did not obtain marked differences in the velocities of centripetal versus centrifugal saccades into the movement field. Also, main sequence fits between amplitude and mean eye velocity were determined for each quadrant (according to *Eq. 4*) for saccades belonging to the center of the movement field (see Fig. 4*A*) and checked for significant differences. Figure 5 shows the result of this latter analysis for the data of *cell cr4603*. Different

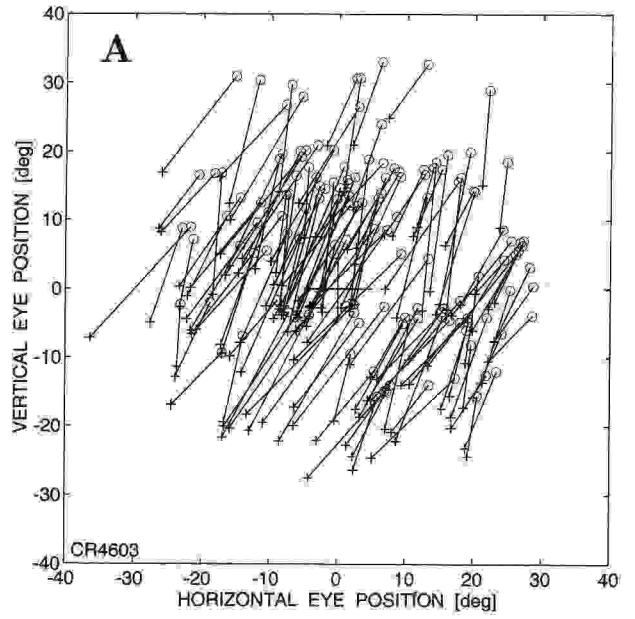

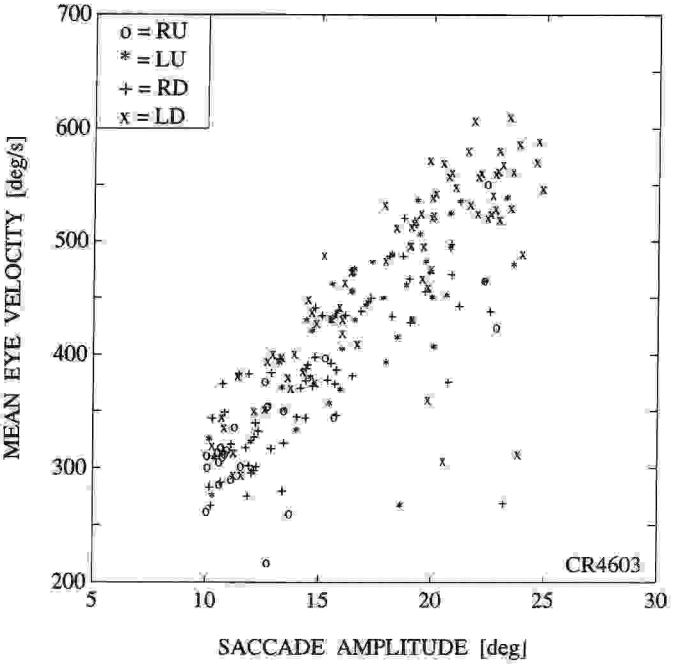

FIG. 5. Main sequence characteristics of the saccades in the optimal metrics bins of Fig. 4*A*. Mean eye velocity is plotted as a function of saccade amplitude. Each eye position sector is identified by a different symbol (see *inset*). Robust regression for the 4 quadrants according to *Eq. 4* yields the following. $R + U$: $\alpha = 199.3°/s$; $\beta = 12.1\ s^{-1}$; $r = 0.64$. $L + U$: $\alpha = 181.0°/s$; $\beta = 15.1\ s^{-1}$; $r = 0.78$. $R + D$: $\alpha = 146.1°/s$; $\beta = 15.8\ s^{-1}$; $r = 0.76$. $L + D$: $\alpha = 160.1°/s$; $\beta = 16.1\ s^{-1}$; $r = 0.86$. Apart from the $R + U$ quadrant, these regression lines are statistically indistinguishable. Thus no systematic dependence on eye position is apparent.

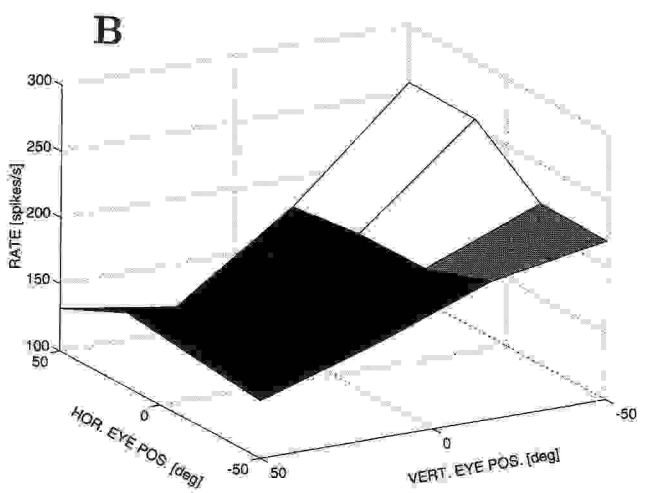

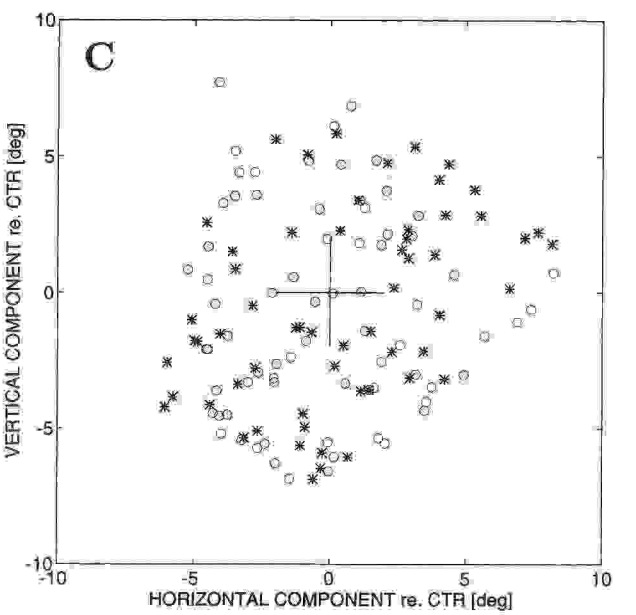

symbols refer to the different eye position quadrants (see *inset*). Note that amplitudes appear to be roughly homogeneously distributed over the 10.0–25.0° range for most sectors (see also below). Although a somewhat larger scatter for mean velocities and smaller correlation coefficient in the top-right quadrant ($R + U$) was obtained, the robust regressions for the other three sectors were statistically indistinguishable (see legend of Fig. 5, for details).

To further quantify the effect of eye position on the activity of this unit, we subjected the complete set of 2,735 saccadic eye movements to the two model descriptions of *Eqs.*

FIG. 4. *A*: saccades are selected in the estimated optimal amplitude/direction bin: $[\Delta R] = [10, 25]$, and $[\Delta\Phi] = [60 \pm 20]$ deg ($N = 132$). Saccade vectors are plotted relative to the center of the oculomotor range as straight lines between onset position (+) and saccade offset position (○). Data from recording of *cr4603*. *B*: qualitative mesh plot of the cell's gain field based on tiling the oculomotor range by a regular 4 × 4 matrix of 20 × 20°, in which neighboring sectors overlap by 25%. Height of each point in the mesh plot is the mean firing rate of saccades belonging to the given eye position sector. Gray code symbolizes intensity of firing. Note that highest firing rates are obtained for initial eye positions in the lower oculomotor range and that there is a gradual decrease in activity for increasing elevations. Multiple regression (*Eq. 1*) on the data of *A* yield: $f_0 = 161$ spikes/s, $f_H = -1.2$ spikes/s/deg, and $f_V = -4.1$ spikes/s/deg [$r = 0.36$, $P(r) < 10^{-6}$]. *C*: saccade vectors relative to the estimated optimal saccade $(R, \Phi) = (16.5, 60)$ deg (indicated by center of the cross), for 2 populations of saccades belonging to 2 equally large nonoverlapping sectors along the fitted gradient of the gain field, $\vec{f}$. Thus open circles indicate saccades of the top half the oculomotor range ($N = 73$), whereas asterisks correspond to saccades of the bottom half ($N = 59$). The 2-dimensional Kolmogorov-Smirnov statistic for these 2 populations, $d = 0.33$, is insignificant, indicating that both saccade populations are statistically indistinguishable.

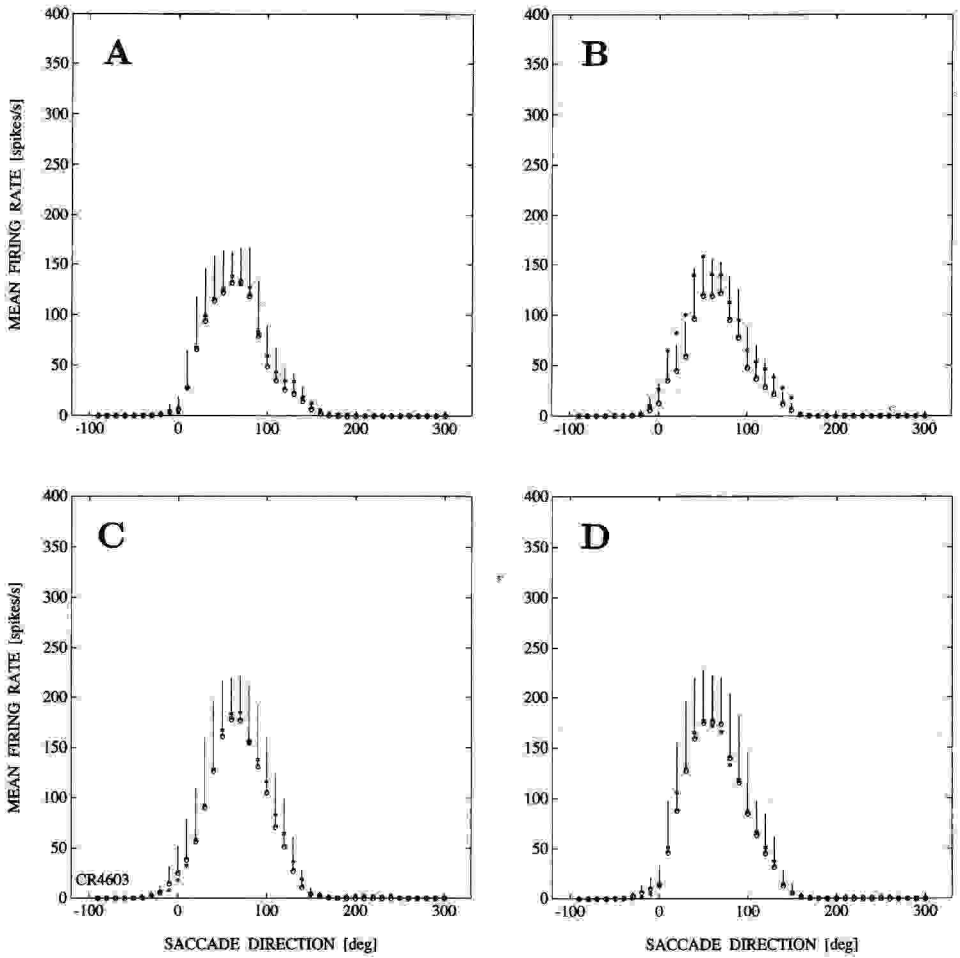

FIG. 6. Result of the gain field fit (*Eq. 2*) for *neuron cr4603*. The 4 panels correspond to directional tuning curves in the 4 quadrants of the monkey's oculomotor range and are plotted in the same format and scaling as Fig. 3. Saccade amplitudes have been selected around the fitted optimal amplitude ($R = 14.6°$), such as to yield at least 75% of the predicted peak firing rate of the cell for saccades in the optimal direction, ($\Phi = 65.5°$), made from $H = V = 0°$. Thus $R \in [9, 23]$ deg. Asterisks correspond to the measured mean firing rate of the cell within the selected amplitude and direction bin. Open circles indicate the prediction of the cell's firing rate for the same population of saccade vectors, based on the fitted parameters of *Eq. 2* (see Table 1). Standard deviations around the predicted mean firing rates are nonzero because of the range of selected amplitudes (14°) and directions (±20°) within each bin (typically ~20 responses/bin). The optimal direction of the cell and the direction of the gradient vector of the fitted planar gain field ($\Psi = 267°$), are approximately in the opposite direction. See text and Table 1 for further details.

2 and *3*. Figure 6 shows the result of fitting the gain field model (*Eq. 2*) to all saccades of Fig. 1, *A* and *B*. The data are displayed in the same format as Fig. 3, so that only the result of the fit for saccades within a restricted amplitude range, defined by 75% of the predicted peak firing rate for saccades from $[H, V] = (0, 0)$, is shown ($R \in [9, 23]$ deg). The open symbols correspond to the predicted average firing rate, whereas upward directed lines are the predicted standard deviations. It is important to note that these standard deviations are now entirely due to the scatter of the saccade vectors within each $[\Delta R, \Delta\Phi]$ bin. Asterisks are the measured mean firing rates for the same saccade vectors, as they are also shown in Fig. 3. Note the good correspondence between fit and data in all four eye position sectors. The linear correlation coefficient between predicted and measured firing rate was highly significant ($r_{GN} = 0.75$; $P < 10^{-6}$). The optimal saccade vector obtained by the fit was estimated as $(R, \Phi) = (14.6, 65.3)$ deg, which agrees well with the qualitative observations made above. The optimal motor error tuning width in the collicular motor map is 0.73 mm, and the peak firing rate from the center of the oculomotor range $F_0 = 199$ spikes/s. These values are close to those typically reported in earlier studies (Stanford and Sparks 1994; Ottes et al. 1986; Van Opstal et al. 1990). However, the most important distinguishing feature of the model is the gain field modulation vector, $\vec{a}$, which was determined as $(a, b) = (-0.4, -3.8)$ spikes/s/deg. The direction of this eye position gradient vector equals $\Psi = 267.0°$ and is almost opposite to the cell's optimal direction ($\Delta\Phi \approx 202°$). Note that this direction corresponds well to the gradient that was obtained by linear regression on optimal saccades only (Fig. 4*B*). Thus also the gain field model of *Eq. 2*, applied to the entire data set of 2,735 saccades, predicts that *cell cr4603* has an *anti-linear gain field* and that its strength is 3.8 spikes/s/deg.

The result of fitting the data to the classical movement field function of *Eq. 3* is shown in Fig. 7. Despite the high correlation between predicted and measured firing rate ($r_{CL} = 0.72$; $P < 10^{-6}$), this model appears to deviate in a systematic way from the measured values. In the upper eye position sectors the fit overestimates the measured firing rates, whereas for the lower sectors the data are underestimated. The difference between the two correlation coefficients was found to be highly significant [$P(\text{diff}) < 10^{-6}$].

It is important to note that the predicted peak value of the classical model fit for measured saccades in each eye position sector reaches the same value of ~163 spikes/s. This is even true for the saccades in the top-right quadrant. As we have argued in METHODS, this indicates once more that the eye position dependence, observed by qualitative inspection of Figs. 3 and 4, cannot be explained by systematically different distributions of saccade vectors in the four eye

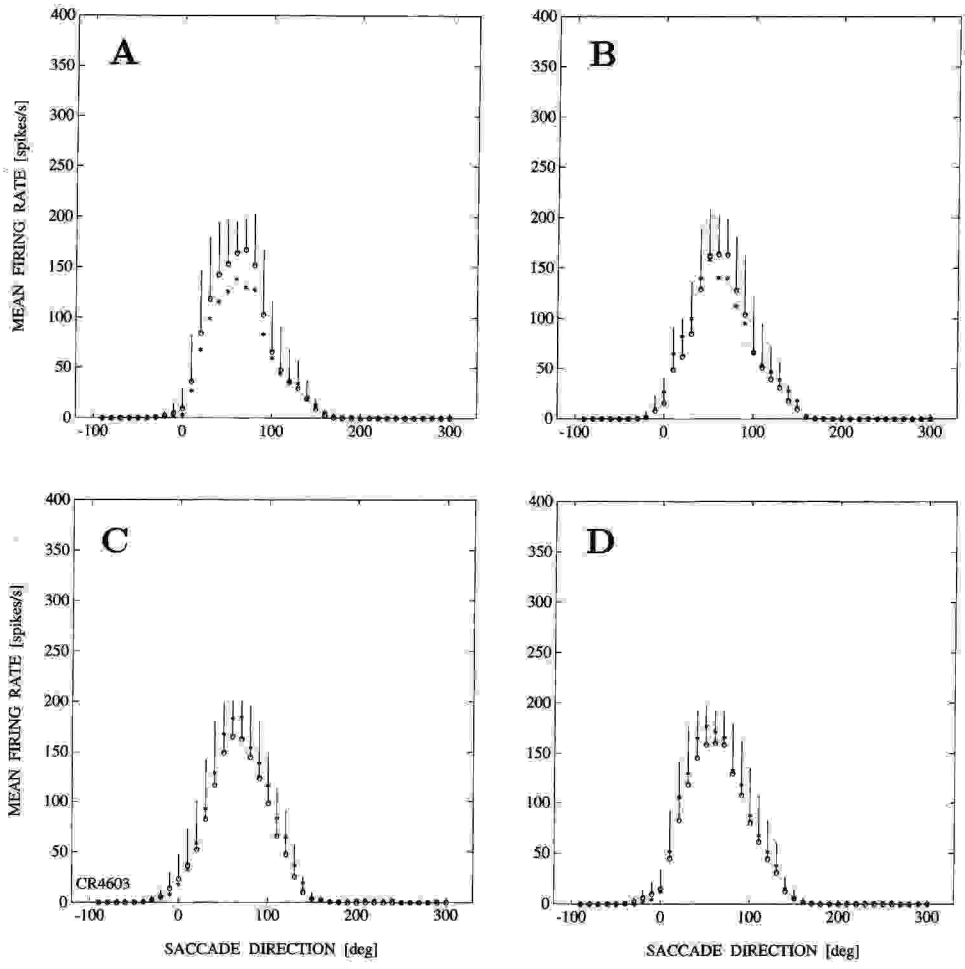

FIG. 7. Same cell as in Figs. 1–6, but now a fit has been applied according to *Eq. 3*, assuming no gain field modulation. Note, that in this case, the data deviate systematically from the prediction of the optimal fit function. The upper eye position sectors are systematically overestimated, whereas the lower sectors are underestimated by the fit function. Predicted peak firing rate within every quadrant is roughly constant at ~163 spikes/s. This indicates that differences in the amplitude and direction distributions of the 4 eye position sectors (see, e.g., Fig. 2) cannot explain the observed modulation of average peak firing rate by eye position. For optimal fit parameters, see Table 2.

position quadrants. Note that the optimal values of the parameters $[u_0, v_0, F_0, \sigma_p]$ are in good agreement for both models (see legends to Figs. 6 and 7 and Tables 1 and 2). This strongly suggests that the significant improvement of fitting the data by *Eq. 2* is obtained by including the parameters (a, b) in the model's description.

To further assess the statistical significance of the fitted values of gain field vector $\vec{a}$, a bootstrap simulation was run on the neuron (see METHODS). Figure 8 shows the resulting parameter distributions of a and b for four identified gain field neurons. In all four cases, either one or both gain field parameters differ significantly from zero by at least two standard deviations (see legend and Table 1).

On the basis of the fitted gain field vector $\vec{a} = (a, b)$ of *Eq. 2*, we considered an additional check on the eye position effect. A planar gain field modulation indicates that one should expect a significant and maximal increase in the cell's mean firing rate for initial eye position components parallel to the fitted eye position gradient vector. To investigate this prediction quantitatively, the following procedure was followed. First, all saccades belonging to the bin around the optimal vector (for cell *CR4603:* $R \in [9, 23]$, $\Phi \in [65 \pm 20]$ deg) were selected ($N = 141$). Then, for each saccade, i, the component of initial eye position parallel to the normalized gradient vector $a_n = (\vec{a}_n, b_n) = \vec{a}/\sqrt{a^2 + b^2}$, was computed according to

$$E_i^{\parallel} = H_i \cdot a_n + V_i \cdot b_n \qquad (5)$$

Figure 9*A* shows the mean firing rate for the individual saccades as a function of $E_i^{\parallel}$. The correlation coefficient between $E^{\parallel}$ and $\bar{F}_{dyn}$ is significant [$r = 0.30$; $P(r) < 10^{-4}$]. The *inset* displays the direction of the fitted gain field gradient vector, $\vec{a}$ (*) and the direction of the optimal saccade vector (○). Linear regression yields a line with a slope of 3.6 spikes/s/deg, which is quite comparable with the value of 4.1 spikes/s/deg found by the multiple regression analysis presented in Fig. 4, and the value of 3.8 spikes/s/deg found by fitting the entire data set of 2,735 saccades (see Fig. 6). Note that mean eye velocity of the selected saccades as a function of $E^{\parallel}$ has only a very weak correlation [$r = 0.12$; $P(r) = 0.04$; *bottom* of Fig. 9*A*]. In line with the observations made above, this indicates once again that the increase in firing rate along the gradient of the fitted gain field vector cannot be attributed to systematic changes of saccade velocity.

In Fig. 9*B*, the individual spike trains corresponding to the selected saccades have been ranked as a function of the corresponding $E_i^{\parallel}$ component. The *right-hand side* of this panel shows the histogram of mean firing rate during the saccade as a function of $E_i^{\parallel}$. Although not immediately obvious from the spike trains, a systematic decrease of mean firing rate with decreasing $E_i^{\parallel}$ can nevertheless be observed. The cumulative histogram at the *bottom of this panel* shows

TABLE 1. *Gain field fit results*

Unit	a	b	F_0	R	Φ	σ_p	N	r	Type
cr2506	−0.06	2.34	207	39.8	104.9	1.11	2,050	0.71	C
cr3002	−14.23	−5.42	866	10.0	104.3	0.48	1,426	0.87	O+
cr4403	−2.24	3.43	268	19.5	74.6	0.48	2,991	0.76	C
cr4404	−0.26	6.08	659	27.7	72.7	0.88	1,633	0.90	C
cr4405	2.64	9.52	668	45.4	64.0	1.12	3,920	0.76	C
cr4501	−0.35	8.90	314	22.2	77.6	0.48	2,042	0.59	C
cr4502	0.32	9.13	733	25.8	62.7	0.66	1,332	0.90	C
cr4504	4.29	5.59	559	29.8	54.1	0.75	2,745	0.85	C
cr4601	−1.05	4.46	268	14.2	86.2	0.37	952	0.78	C
cr4603	−0.38	−3.79	199	14.6	65.3	0.73	2,735	0.75	A
cr4902	3.64	2.80	135	32.8	171.2	0.87	1,642	0.49	A
cr5002	0.53	2.92	141	36.2	96.3	0.75	2,812	0.49	C
cr5301	6.66	2.14	738	9.4	84.6	0.54	4,534	0.78	O−
cr5302	8.59	0.77	731	10.3	85.0	0.56	4,303	0.84	O−
cr5404	6.62	−3.28	443	4.1	103.4	0.75	5,878	0.67	A
cr6001	−1.21	4.51	764	19.2	125.1	0.86	3,670	0.92	C
yu1302	1.42	−0.21	138	29.2	68.5	1.45	2,892	0.78	O−
yu1503	−5.91	−9.19	683	3.6	75.4	0.45	3,199	0.83	A
yu1603	−0.21	−1.24	146	16.0	66.8	1.23	2,136	0.53	C
ca0804	−1.82	0.42	232	8.6	111.3	0.85	1,335	0.85	C
ca0901	1.37	0.02	152	17.4	88.7	0.66	431	0.79	O−
ca0902	1.83	0.74	163	16.5	74.4	0.77	756	0.68	C
ca1502	9.68	1.27	284	14.0	210.2	0.45	2,069	0.65	A
ca1803	−0.19	2.00	142	31.7	105.0	0.95	1,446	0.74	C
ca8905	−3.91	−1.20	273	11.9	224.2	0.77	745	0.78	C
ca8909	7.01	−2.14	587	2.5	198.3	0.40	838	0.88	A
ca9002	1.23	1.03	201	8.4	67.9	0.97	1,373	0.79	C
ce3101	2.61	7.12	321	8.0	56.8	0.97	1,588	0.72	C
ce3102	−1.50	5.33	270	9.3	50.2	0.85	660	0.64	C
ce5101	6.97	−3.28	326	4.6	50.5	0.62	961	0.77	O−

Parameters of fitting the model of *Eq. 2* to the complete data set for each cell, which had a significant gain field ($N = 30$).

the presaccadic burst associated with the saccades into the movement field.

As an important check for the existence of a planar gain field, no significant relation should emerge if mean firing rate is plotted as a function of the component of eye position *perpendicular* to the gain field gradient, i.e.

$$E_i^{\perp} = -H_i \cdot b_n + V_i \cdot a_n \qquad (6)$$

The result of this analysis, in the same format as Fig. 9*A*, is shown in Fig. 9*C*. In this case the correlation coefficient is indeed insignificant [$r = -0.09$; $P(r) = 0.38$; slope of the linear regression line is −0.9 spikes/s/deg]. Also the spike trains, when ranked as a function of $E_i^{\perp}$, no longer display the systematic dependence of eye position as in Fig. 9*B* (not shown). Mean velocity now tends to decrease with $E^{\perp}$ [$r = -0.42$; $P(r) < 4.10^{-5}$; *bottom figure*] but cannot be related to the behavior of the cell's firing rate as a function of this parameter.

In summary, we considered a cell to display a significant planar gain field when its behavior obeyed all of the criteria outlined above.

1) A significantly better correlation coefficient for the fit of *Eq. 2* than for *Eq. 3* (Figs. 6 and 7). In addition, the highest correlation coefficient should exceed $r = 0.70$. Thus at least 50% (r^2) of the variability in the data should be explained by the model description.

2) No "false" gain field when the prediction of the firing rates is made according to *Eq. 3* (Fig. 7).

3) A significant relation for the analysis according to *Eq. 5*, but no significant relation for *Eq. 6* (Fig. 9).

4) Statistically significant components of $\vec{a}$ according to the bootstrap simulation (Fig. 8), in the sense that at least one of the components should differ from zero by at least two standard deviations.

5) No systematic differences for saccade velocities into the center of the movement field, elicited from the different eye position sectors (Figs. 5 and 9).

6) Sufficient numbers of saccades within the selected amplitude range, equally distributed over the various eye position quadrants (Figs. 1*C* and 2);

7) Consistent alignment for the eye position modulation vectors found by the model-free method, $\vec{f} = (f_H, f_V)$ of *Eq. 1*, and by the model description of the collicular motor map, $\vec{a} = (a, b)$ of *Eq. 2* (Figs. 4*B* and 6).

In all cases, the significance level for rejection was taken at $P > 0.05$. Table 1 provides the results of the gain field fits (*Eq. 2*) for our complete sample of identified gain field neurons. Table 2 shows the results of the fit of *Eq. 3* for the same population of neurons.

A total number of 22 of 57 cells (39%) meet all of these criteria. If no restrictions are imposed on the strength of the correlation coefficient for the gain field model, even 30 cells (59%) appeared to meet our criteria (see Table 1). In Fig. 10 an attempt is made to characterize the entire population of 22 gain field neurons. Figure 10*A* displays the distribution of the mean horizontal and vertical gain field gradient com-

TABLE 2. *Classical movement field fit results*

Unit	F_0	R	Φ	σ_p	r	$P(r_{GN} > r_{CL})$
cr2506	173	37.1	106.5	1.14	0.70	0.014
cr3002	779	9.9	103.6	0.50	0.84	*
cr4403	254	19.1	73.9	0.48	0.74	*
cr4404	584	25.9	71.9	0.88	0.88	†
cr4405	484	38.9	61.7	1.14	0.73	*
cr4501	257	21.5	78.0	0.46	0.53	*
cr4502	701	26.1	63.6	0.65	0.88	†
cr4504	454	27.9	54.8	0.76	0.83	*
cr4601	250	13.8	86.3	0.37	0.76	0.008
cr4603	218	15.2	65.4	0.74	0.72	*
cr4902	224	36.7	173.8	0.79	0.47	0.017
cr5002	93	31.3	97.6	0.77	0.45	*
cr5301	770	9.3	83.8	0.52	0.76	*
cr5302	748	10.3	83.7	0.55	0.81	*
cr5404	377	3.4	99.1	0.89	0.62	*
cr6001	726	18.5	125.5	0.86	0.92	0.005
yu1302	137	28.9	73.6	1.44	0.76	†
yu1503	637	3.5	75.0	0.46	0.81	*
yu1603	153	17.9	66.2	1.23	0.52	0.04
ca0804	243	8.5	111.0	0.83	0.84	0.004
ca0901	149	18.2	88.3	0.67	0.76	0.018
ca0902	154	15.9	76.2	0.75	0.65	0.005
ca1502	289	14.4	211.9	0.50	0.60	*
ca1803	112	28.7	105.0	0.96	0.73	0.004
ca8905	246	11.0	225.2	0.78	0.75	†
ca8909	608	2.5	201.2	0.40	0.86	*
ca9002	196	8.1	67.0	0.97	0.78	0.033
ce3101	333	7.2	58.1	0.93	0.67	*
ce3102	283	8.7	48.6	0.85	0.61	0.025
ce5101	350	4.5	45.8	0.61	0.74	†

Parameters of fitting the model of *Eq. 3* to the complete data set for all cells of Table 1. Significance of difference in correlation coefficients: *$P < 10^{-6}$; †$P < 10^{-4}$.

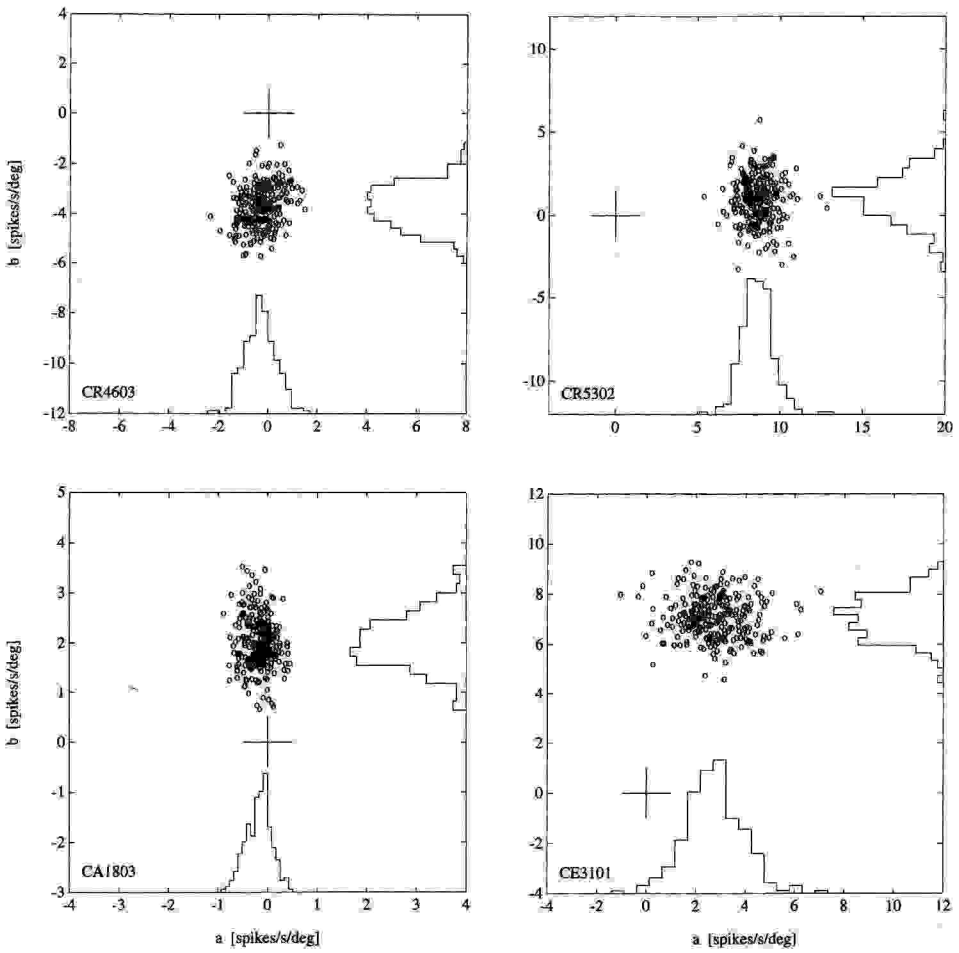

FIG. 8. Results of the bootstrap simulation (see METHODS) for 4 different neurons (identified in panels) in order to determine the confidence limits of the gain field modulation vector $\vec{a}$. See also Table 1 for further details.

ponents (μ_a, μ_b), with their 68% confidence intervals (σ_a, σ_b) (all in spikes/s/deg) as determined by the bootstrap method. Note that the obtained gradient vectors scatter widely over all directions and amplitudes.

In Fig. 10*B* the gradient vectors are plotted relative to the fitted optimal motor error direction of the cell, by determining their difference angle, $\Delta\Phi = \psi - \Phi$. In this plot the solid lines correspond to the length of each gain field vector ($\|\vec{a}\| = \sqrt{a^2 + b^2}$). The four diagonal sectors may roughly characterize the gain field gradients as colinear vectors (C), antilinear vectors (A), or orthogonal vectors (O+, O−), respectively. In our sample of neurons, the majority (13/22) falls within the colinear (11/13)/antilinear (2/13) cones, whereas 9/22 neurons have orthogonal gain field directions. The correlation between gain field direction, ψ, and optimal motor error direction, Φ, is not significant ($r_{\psi\Phi} = 0.32$; $P > 0.05$). The relative proportions of these gain field types do not appear to be very sensitive to the set of criteria imposed above. For example, when we alleviate the demand $r_{GN} \geq 0.70$, these relative numbers are for C type: 17/30; A type: 4/30; and O type: 9/30, respectively.

DISCUSSION

General summary

A substantial portion of our total sample of neurons (22/57) could be described by planar gain fields, which suggests the presence of an eye position signal at the level of the collicular motor map. It appeared that the tuning of the cells does not change as a function of eye position, because in all cases the peak activity occurred for saccades having similar vectors all over the oculomotor range. However, the height of this peak activity was found to be modulated by eye position in a similar way as has been described for neurons in monkey posterior parietal cortex (Andersen et al. 1985, 1990). Often, however, the shape of this modulation could be quite complex, both in parietal cells, as well as for a number of collicular cells in our sample. In this study we have provided a first-order approximation of this phenomenon by the planar gain field description.

We believe that the observed effects are not caused by the use of vestibular stimulation. First of all, as is shown for the neuron depicted in Figs. 3–8, the gain field persists when only eye movement data are taken that were generated without a vestibular stimulus. In fact, the cell's gain field parameters did not change for either experimental mode. Second, in an earlier paper we have shown that vestibular stimulation with a prominent torsional component does not have a significant influence on the firing of collicular neurons (Hepp et al. 1993). Indeed, that study indicated that the collicular code could best be described by a desired eye displacement vector, $\vec{d}$, within Listing's plane. This conclusion was corroborated by electrical microstimulation that always yielded saccadic displacements within this plane

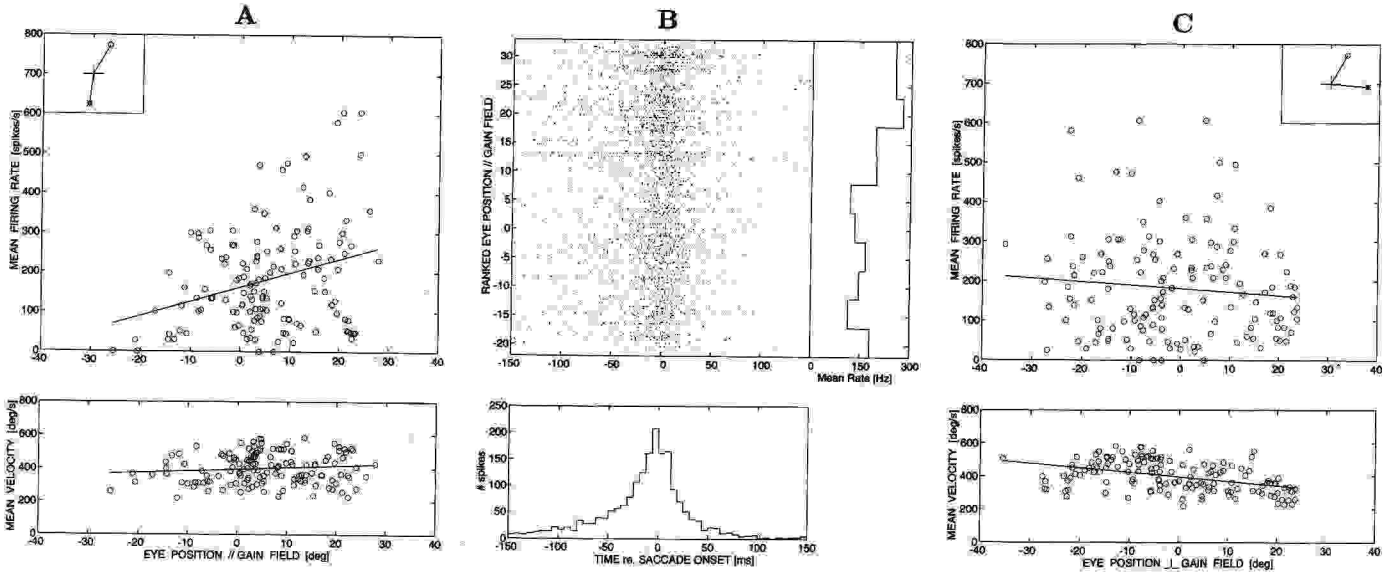

FIG. 9. Firing rate of saccades into center of the movement field. *A*: saccades are selected in the optimal $[\Delta R, \Delta\Phi]$ bin, resulting from *Eq. 2* ($N = 141$). *Top panel*: mean firing rate for individual saccades as a function of their initial eye position component along the fitted gain field gradient vector, $E^{\parallel}$ (see *Eq. 5*). Despite the high variability in the cell's activity, which is due to both the scatter in saccade metrics and intrinsic variability of the cell, high firing rates tend to coincide with high values of $E^{\parallel}$. The correlation between these 2 variables is highly significant [$r = 0.30$, $P(r) < 10^{-5}$]. The regression line has an intercept at $\bar{F} = 162$ spikes/s and a slope of 3.6 spikes/s/deg. Note that these values agree well with the optimal fit values of *Eq. 2* (see Table 1), which were based on the complete data set of 2,735 saccades. *Bottom panel*: mean eye velocity of the same saccades as a function of $E^{\parallel}$. The correlation coefficient, $r = 0.12$, is significant [$P(r) = 0.04$]. However, the slope of the regression line is very modest. Thus changes in saccadic eye velocity cannot explain the tendency of an increase in mean firing rate with $E^{\parallel}$. *B*: individual spike trains, from 150 ms before to 150 ms after movement onset, for each saccade of *A* have been ranked according to $E^{\parallel}$. The *right-hand side* of this panel shows the cumulative histogram of mean firing rate as a function of $E^{\parallel}$. Note steady decrease of the mean firing rate as $E^{\parallel}$ decreases. The *bottom panel* shows the cumulative spike histogram associated with the saccade. Note that the burst reaches its peak value slightly before saccade onset. *C, top panel*: activity for same saccades as in *A*, now plotted as a function of $E^{\perp}$ (*Eq. 6*). In this case, no significant relation of mean firing rate with $E^{\perp}$ is obtained: $r = 0.04$ [$P(r) = 0.58$]. Regression line: intercept at $\bar{F} = 170.0$ spikes/s; slope -0.4 spikes/s/deg. *Bottom panel*: mean eye velocity. A significant negative correlation is obtained [$r = -0.30$; $P(r) = 4.10^{-5}$]. Note that this behavior cannot be related to the cell's activity.

(Hepp et al. 1993; Van Opstal et al. 1991), irrespective of stimulation site or initial eye position.

Although the present study suggests that collicular activity may be better characterized by a four-parameter description, given by the eye position sensitivity (or gradient) vector $\vec{a} = (a, b)$, and the desired eye displacement vector, $\vec{M} = (R, \Phi)$, both optimal vectors are still confined to Listing's plane. This latter point was supported by the static roll experiments in *monkeys Cr* and *Yu* (see METHODS), during which a static counterroll of the eyes up to $|r_x| \approx 5°$ was obtained. Nevertheless, the cell's behavior was always characterized best by a displacement vector in Listing's plane.

Notice that even the cells with a strong *orthogonal* gain field (e.g., *cr3002* and *cr5302;* see Table 1), showed no significant relation between the mean firing rate of the cell and the torsional component of the saccadic eye displacement vector. This result therefore supports our earlier single-unit findings (Hepp et al. 1993), which indicated that Listing's law is not implemented at the level of single units in the motor SC. Thus the presence of orthogonal gain fields is not in conflict with this view (see also below).

As has been briefly outlined in the INTRODUCTION, several lines of earlier experimental evidence have suggested that the colliculus may have access to an eye position signal. To our knowledge, the present study provides a first systematic attempt to quantify the influence of variation in eye position on the activity of neurons in the monkey colliculus.

Comparison with other studies

Our quantitative analysis indicates that the absolute strength of the gain fields can be quite high: in 13 of 22 gain field neurons, the eye position sensitivity vector exceeded a value of 5 spikes/s/deg. This sensitivity appears to be even higher than the values reported for posterior parietal cortex where the modulation by eye position may be seen to be roughly between 1 and 3 spikes/s/deg (see Andersen et al. 1990). Therefore one must wonder why it was not observed before. Several factors may have contributed to this apparent discrepancy.

First, the activity of collicular neurons is endowed with a substantial amount of noise: the firing rate of a given neuron may vary by tens of percents of the peak firing rate, even for identical saccades into the center of the movement field. Therefore, in order to observe the second-order effect of an eye position modulation, one must measure a large sample of saccadic eye movements, homogeneously covering the full oculomotor range. Indeed, simulations with the gain field model of *Eq. 2* indicate that multiplicative noise in the firing rates of 40% of the peak (which is a reasonable estimate for the amount of noise in a typical collicular neuron) will hide an eye position sensitivity of 3 spikes/s/deg for homogeneously drawn sample sizes below 500 saccades.

Second, the absolute activity of cells in the colliculus can

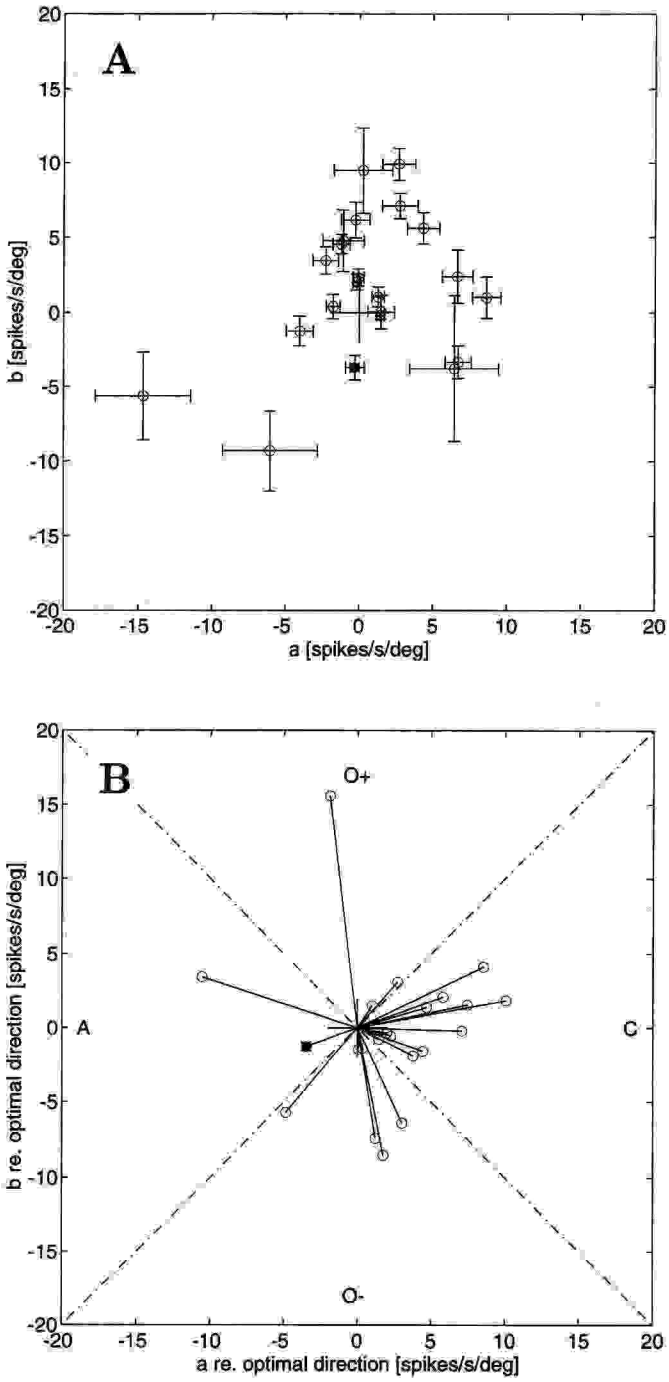

FIG. 10. Gain field sensitivity vectors $\vec{a}$ for all gain field cells of Table 1 with $r_{GN} > 0.70$. Filled symbol corresponds to *cell cr4603*. *A*: mean and estimated standard deviations (based on the bootstrap procedure) of vectors $\vec{a}$ in head-centered Cartesian coordinates. Note wide distribution of amplitudes and directions of gain field vectors. *B*: gain field vectors are replotted with respect to each cell's optimal direction (corresponding to the rightward direction in this panel). Note the wide range of relative gain field directions, although the majority of gain fields tends to cluster in the colinear sector (*C*). Other types: O+ and O−: orthogonal gain fields; *A*: antilinear gain fields.

reach intensities up to ~900 spikes/s (see Table 1). In this respect, the relative effect of eye position is rather modest: if one takes the quotient $g = \|\vec{a}\|/F_0$, which measures the relative contribution of each degree variation in eye position to a cell's firing rate, it appears that $g \approx 1.7\%$/deg. This is in remarkable agreement with the values for LIP neurons reported by Andersen et al. (1990), indicating a modulation depth of 40% of the peak firing rate for eye position variations over a 30° range (cf. their Table 3). The difference in absolute value with our collicular neurons may be due to the lower firing rates of the cortical cells.

In summary, in order to observe a collicular gain field, one needs a large range of eye positions *along* the gain field sensitivity vector (yielding an optimal eye position effect in the order of tens of percents of the peak firing rate) and large numbers of saccades (for filtering out the random noise, which is of the same order).

The first two points are the main reason that casual inspection of the spike trains (see, e.g., Fig. 9*B*) does not readily show the influence of eye position for each saccade.

In most collicular recording studies, the monkey is required to fixate a visual target in an otherwise darkened environment, before the saccade is triggered by a peripheral visual stimulus. In our paradigm, the monkey is encouraged to look around "spontaneously" in the well-lit laboratory room. The saccades are therefore self-generated and not contingent upon reward. It should be noted that the saccades generated by our monkeys had normal main sequence properties and also that the velocity profiles of the saccades and their variability were within normal limits. One potentially important factor that is different for the two paradigms is the involvement of the rostral fixation zone (Munoz and Wurtz 1993). It has been suggested that cells in this zone exert an inhibitory influence on the saccade-related burst neurons during fixation. However, when the monkey is not engaged in active fixation, as is the case in the spontaneous visuomotor paradigm, the rostral fixation cells are practically silent (Munoz and Wurtz 1993). Thus the excitability of cells in the motor SC may be substantially different for the two experimental paradigms, and it is possible that the inhibitory fixation mechanism may further mask the second-order influence of the eye position signal.

Although the significance of the gain field in three cells vanished when the activity was quantified in the fixed time window around saccade onset (N_{fix}), almost identical gain field results were obtained in the far majority of cells. The result of this analysis is shown in Fig. 11, where the gain field parameters a and b are compared for the fit on F_{dyn} versus F_{fix}. Thus it appears that the manner of spikes counting is not a prominent factor in the emergence of these gain fields.

Possible neurophysiological interpretations

DYNAMIC INTERPRETATION. A majority of gain fields in our sample of neurons (50%) appeared to have the gradient vector roughly aligned with the direction of the optimal saccade displacement vector. The possible function of such colinear gain fields could be related to a dynamic interpretation. Suppose that, for eccentric eye positions, stronger elastic forces need to be overcome than for more central eye positions, because of an increase in the spring constant of the extraocular muscles. Then, if an equally fast and accurate saccadic eye movement is made from a peripheral fixation position toward an even further eccentric eye posi-

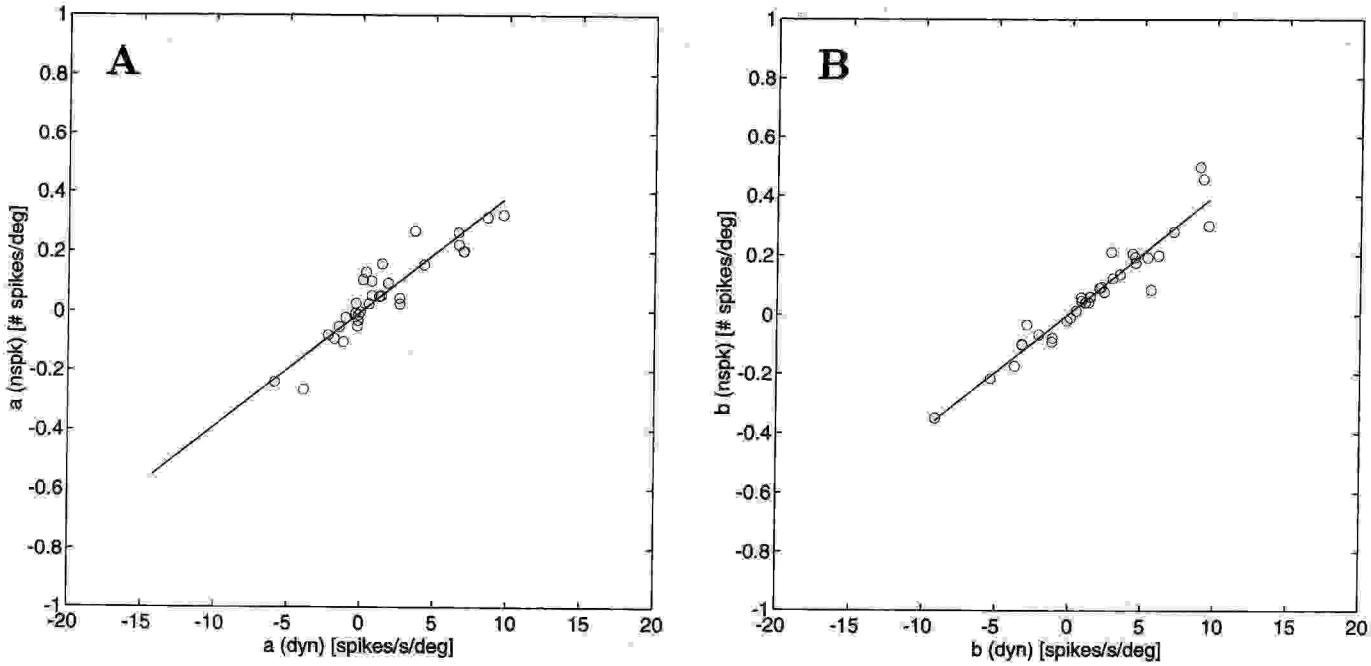

FIG. 11. Fit results of the gradient vector, $\vec{a}$, for all gain field cells of Table 1, compared for 2 different spikes criteria: $\vec{F}_{dyn}$ vs. $\vec{N}_{fix}$. Note the high correlation between the results of the 2 measures, indicating the robustness of the gain field description.

tion, more innervation of the plant is needed than from central fixation points. Such a need for dynamic compensation might be reflected in collicular neurons as a colinear gain field modulation, provided these neurons are part of the control signal that specify saccade kinematics. Indeed, as is summarized in the INTRODUCTION, recent evidence suggests such a role for the colliculus (Berthoz et al. 1986; Lee et al. 1988; Van Opstal and Van Gisbergen 1990; Waitzmann et al. 1991). However, the presence of gain fields orthogonal to the cell's optimal direction (41%), or even oppositely directed (antilinear) gain fields (9%), like the example *neuron cr4603*, cannot be readily accounted for by this dynamic hypothesis.

INCOMPLETE GAZE COMMAND. The motor SC has been implicated in the coordination of both eye and head movements, by sending a common gaze-displacement signal to these motor systems (gaze = eye-in-space). Indeed, electrical stimulation in the SC of the head-free cat yields coordinated eye-head saccades (e.g., Roucoux et al. 1980), whereas the gaze perturbations evoked by SC stimulation in the dark are fully compensated by the first subsequent eye-head saccade (Pelisson et al. 1989). Because in our experimental setup the monkey's head is restrained, it should be considered whether the observed gain fields could be due to an incomplete expression of the collicular gaze command. There are at least three reasons that are inconsistent with such an explanation. First, one would expect a systematic bias in the distribution of saccade vectors as a function of initial eye position, because, in certain parts of the oculomotor range, the unrestrained monkey would tend to generate a head movement more likely than in other parts. This would result in an eye position dependence of saccade amplitude that, however, was not observed over a large part of the oculomotor range (e.g., Figs. 4*A* and 5). Second, because eye and head make well-coordinated movements during gaze shifts, gain fields should all be approximately colinear. As is explained above, gain field directions were rather homogeneously distributed with respect to the optimal motor error vector. Third, one would expect that the strength of the gain field would be proportional to the gaze amplitude vector, because head movements predominantly occur for large-amplitude gaze displacements (Roucoux et al. 1980). We found, however, that the correlation between $\|\vec{a}\|$ and the amplitude of the optimal motor error vector was insignificant ($r = -0.16$; $P > 0.1$; see also Table 1).

GRADUAL TRANSFORMATION. Following the visuomotor pathway for saccade generation, one moves from purely visual areas to exclusively premotor and motor nuclei. However, along this pathway, several regions have now been implicated to carry a mixed code, in which visual receptive fields appear to be modulated by oculomotor input. Gain fields have now been described for posterior parietal cortex (areas 7a, and LIP) (Andersen et al. 1990) and visual area V3a (Galletti and Battaglini 1989), and even receptive fields of cells in the LGN (Lal and Friedlander 1990) and primary visual area V1 (Weyand and Malpeli 1993) have recently been reported to be influenced by eye position in much the same way as has been found in parietal cortex.

It is conceivable that the SC reflects its position between the visual and the motor areas of this pathway, by carrying an increasing amount of motor-related signals, mixed with a purely sensory code. The presence of these eye position signals may thus not constitute any specific functional role.

TARGET REPRESENTATION. Although there appears to be a predominance of colinear gain fields in our sample of gain field neurons, a substantial portion of the cells display gain fields in quite different directions (see Fig. 10*B*). If one supposes that the underlying distribution of eye position sen-

sitivity vectors with respect to a neuron's ON direction contains at least *two independent* directions, it is interesting to consider a different hypothesis on the possible functional role of collicular gain fields (Van Opstal and Hepp 1995).

The recorded population of 57 neurons consists of roughly two equal classes of cells: cells with and cells without a significant gain field. In our hypothesis, the entire population of cells, with and without a gain field, is proposed to embody a collicular output code that reflects both an *oculocentric motor error* signal, as well as a desired position of the eyes in a *craniocentric code*.

The craniocentric signal, which is directly sent to the brain stem saccade burst generator, was already proposed almost two decades ago by Robinson (1975), but so far no evidence for a head-centered target representation feeding directly into the brain stem has been provided. In fact, studies of the collicular role in saccade generation had rather suggested the fixed-vector nature of its output code, which has led to several revisions of the original Robinson scheme (e.g., Jürgens et al. 1981; Scudder 1988; Waitzman et al. 1991). In these revised schemes, the colliculus transmits a desired eye displacement signal.

However, there are several reasons why relying only on displacement signals relative to the fovea may not be an optimal solution for the class of problems with which the saccadic system is faced.

First, in displacement models, the target must be continuously updated after each saccade in order to maintain spatial accuracy (Goldberg and Bruce 1990). If, on the other hand, the target would be stored in a head-centered reference frame, a target remapping needs to be done only once (from a retinal representation into a craniocentric code). After this remapping stage, every eye movement automatically yields the coordinates of the next motor error vector of the target, independent of the number of intervening eye movements. If the remapping process is endowed with noise, the overall accuracy of a goal-directed saccade after several intervening saccades would not deteriorate in the latter model (apart from inaccuracy imposed by a "leaky" memory over longer time scales), whereas displacement models would yield rapidly increasing errors.

Second, saccades can also be directed quite accurately toward auditory and somatosensory defined stimuli. This requirement makes a retinocentric update mechanism a rather cumbersome one.

Parietal neurons have been hypothesized to play a role in the neural transformation of target position from a retinotopic to a craniocentric code (Zipser and Andersen 1988). In area LIP, a considerable proportion of the neurons has been reported to possess a gain field, whereas motor error encoding has also been found in this region. These neurons are known to project to the SC. Because infinitely many combinations of motor error and eye position signals can give rise to the same desired eye position signal in the head, the latter cannot be reconstructed from gain fields when there would only be colinearity. One would need at least two independent directions of eye position modulation to be able to reconstruct the desired eye position vector. Thus, in principle, all possible eye position modulation vectors re to the optimal displacement vector would be expected in such a scheme. For any given desired eye displacement code, and given eye position, a specific weighting of the gain field population activity may signal the correct target vector to downstream circuits. In this way, the same output population of neurons may in fact send simultaneously two different signals to the pulse generator (an oculocentric and a craniocentric code) and both may be operative during saccades. In Fig. 12, a conceptual diagram of the proposed model is presented.

Recently, the properties of a quantitative neural network model that incorporates these concepts have been studied (Van Opstal and Hepp 1995). Our results indicate that a population of gain field neurons, with randomly distributed eye position sensitivity vectors and with modulation strengths comparable with the ones found in this study, is indeed capable of encoding both an accurate representation of desired motor error, as well as a desired eye position in head-centered coordinates. Indeed, we have also shown that, in principle, such a scheme may effectively encode the desired rotation axis of the eye in three dimensions.

APPENDIX: FIT PROCEDURE OF MOVEMENT FIELDS

We have applied the afferent mapping function as described by Ottes et al. (1986) and Van Opstal et al. (1990) in order to relate the saccade vector $(x, y) = [R \cos(\Phi), R \sin(\Phi)]$ (in deg) to anatomic coordinates (u, v) (in mm). In this latter coordinate system, the activity distribution in the motor map may be described by a rotation-symmetrical Gaussian in good approximation. However, a problem with this simple description arises when movement fields of saccade-related burst neurons are close to the vertical meridian representation, because in that case, the activity is divided over two, anatomically separated, colliculi. To overcome this problem, we have applied the following procedure.

1) On the basis of our qualitative plot of the direction-dependent tuning curves of the cell under study (see, e.g., Fig. 3), the optimal direction of the cell's movement field, Φ_{opt}, was estimated as the mean of the direction bins for each eye position sector where mean firing rate reached its peak value.

2) We then performed a *clockwise* rotation on the saccade vectors over Φ_{opt} deg, so that in this rotated system, the estimated optimal direction coincided with $\Phi = 0°$ (i.e., rightward)

$$x' = \cos \Phi_{opt} \cdot x + \sin \Phi_{opt} \cdot y \tag{A1}$$

$$y' = -\sin \Phi_{opt} \cdot x + \cos \Phi_{opt} \cdot y \tag{A2}$$

3) Subsequently, the collicular coordinates, (u', v'), for the rotated saccade components, (x', y'), were computed by applying the complex logarithmic afferent mapping function of the motor SC

$$u' = \pm B_u \cdot \ln \frac{\sqrt{(|x'| + A)^2 + y'^2}}{A} \tag{A3}$$

$$v' = B_v \cdot \arctan \frac{y'}{|x'| + A} \tag{A4}$$

where $u' < 0$ for $x' < 0$ (leftward saccades). B_u and B_v are collicular magnification factors and were taken from the literature: $B_u = 1.4$ mm, and $B_v = 1.8$ mm/rad, respectively. A is a scaling constant, $A = 3.0°$ (see Ottes et al. 1986, for details).

4) Because the saccades for which the cell fires are now all distributed around the $v = 0$, $u > 0$ representation, the disconnected nature of the colliculus no longer comes into play.

5) Then *Eqs.* A2 and A3 were applied to the data and, after the iteration procedure had found the minimum χ^2 solution, the inverse

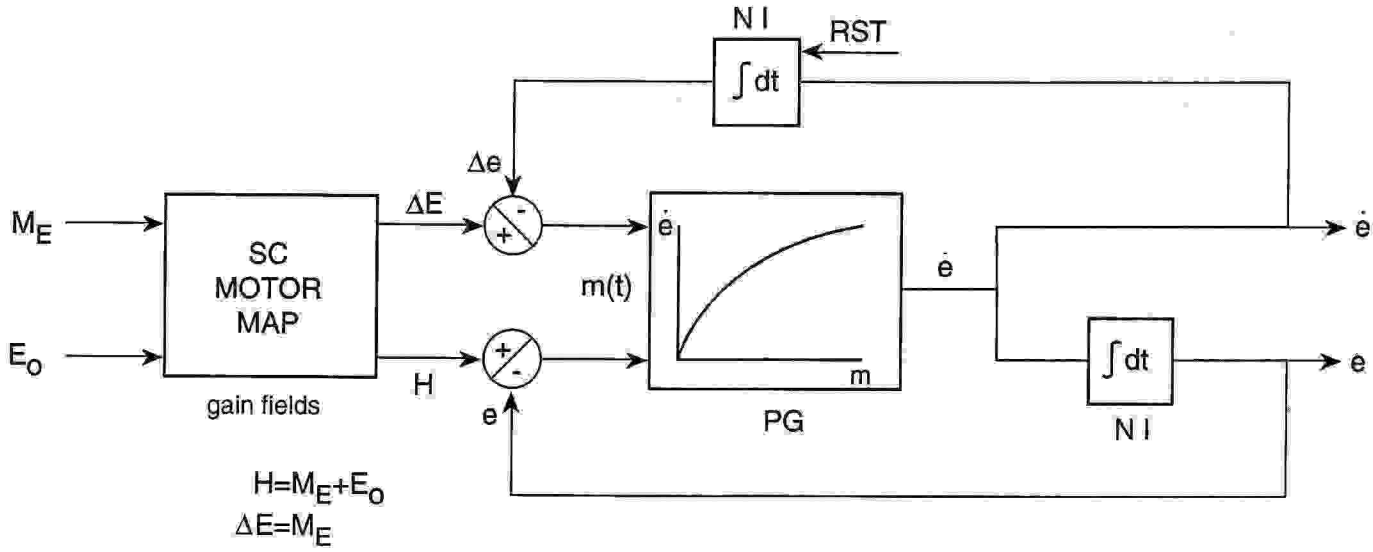

FIG. 12. Conceptual model for the dual code of the collicular motor map. The motor map has access to an initial motor error signal, M_E, as well as to initial eye position, E_0. From the resulting Gaussian population activity profile, where cells embody gain fields with randomly distributed eye position sensitivity vectors, both a desired eye displacement signal, ΔE, as well as a desired eye position signal in head-centered coordinates, H, can be simultaneously extracted by weighted projections to the saccade pulse generator (PG). Local feedback loops ensure that the short lead burst neurons are driven by dynamic motor error, $m(t)$, which is either computed by the difference between ΔE and current eye displacement, Δe (as in recent displacement models), or by the difference between the desired eye position signal, H and current eye position, e (as in the original Robinson model). Note that both feedback loops may operate simultaneously.

mapping formulas of *Eqs. 2* and *3* were used to relate u_0' and v_0' to eye movement coordinates x_0' and y_0', respectively (see also Ottes et al. 1986)

$$x_0' = \pm A \cdot \left| \exp\left|\frac{u_0'}{B_u}\right| \cdot \cos\left(\frac{v_0'}{B_v}\right) - 1 \right| \quad (A5)$$

$$y_0' = A \exp\left|\frac{u_0'}{B_u}\right| \sin\left(\frac{v_0'}{B_v}\right) \quad (A6)$$

with $x_0' < 0$ for $u_0' < 0$.

6) Finally, these parameters were rotated *anticlockwise* over Φ_{opt} deg in order to get the optimal saccade components, (x_0, y_0), in the original coordinate system

$$x_0 = \cos \Phi_{opt} \cdot x_0' - \sin \Phi_{opt} \cdot y_0' \quad (A7)$$

$$y_0 = \sin \Phi_{opt} \cdot x_0' + \cos \Phi_{opt} \cdot y_0' \quad (A8)$$

We acknowledge the assistance of Dr. D. Straumann in the experiments and thank Dr. B. J. M. Hess for manufacturing and implanting the 3D eye coils in the monkeys. We also thank V. Furrer for invaluable care of the monkeys.

This work was supported by the University of Nijmegen (A. J. Van Opstal), the ESPRIT program Mucom II (6615), and the Swiss National Foundation (31.31963.91).

Address for reprint requests: A. J. Van Opstal, University of Nijmegen, Dept. of Medical Physics and Biophysics, Geert Grooteplein 21, NL-6525 EZ Nijmegen, The Netherlands.

Received 28 November 1994; accepted in final form 22 May 1995.

REFERENCES

ALBANO, J. E. AND WURTZ, R. H. Deficits in eye position following ablation of monkey superior colliculus, pretectum, and posterior-medial thalamus. *J. Neurophysiol.* 48: 318–337, 1982.

ANDERSEN, R. A., BRACEWELL, R. M., BARASH, S., GNADT, J. W., AND FOGASSI, L. Eye position effects on visual, memory, and saccade-related activity in areas LIP and 7a of macaque. *J. Neurosci.* 10: 1176–1196, 1990.

ANDERSEN, R. A., ESSICK, G. K., AND SIEGEL, R. M. Encoding of spatial location by posterior parietal neurons. *Science Wash. DC* 230: 456–458, 1985.

BAHILL, A. T., ADLER, D., AND STARK, L. Most naturally occurring human saccades have magnitudes of 15 degrees or less. *Invest. Ophthalmol.* 14: 468–469, 1975.

BAIZER, J. S., DESIMONE, R., AND UNGERLEIDER, L. G. Comparison of subcortical connections of inferior temporal and posterior parietal cortex in monkeys. *Visual Neurosci.* 10: 59–72, 1993.

BERTHOZ, A., GRANTYN, A., AND DROULEZ, J. Some collicular efferent neurons code saccadic eye velocity. *Neurosci. Lett.* 72: 289–294, 1986.

CANNON, S. C. AND ROBINSON, D. A. Loss of the neural integrator of the oculomotor system from brain stem lesions in monkey. *J. Neurophysiol.* 57: 1383–1409, 1987.

CHERON, G., GODAUX, E., LAUNE, J. M., AND VANDERKELEN, B. Lesions in the cat prepositus complex: effects on the vestibulo-ocular reflex and saccades. *J. Physiol. Lond.* 372: 75–94, 1986.

EFRON, B. AND TIBSHIRANI, R. Statistical data analysis in the computer age. *Science Wash. DC* 253: 390–395, 1991.

FRIES, W. Cortical projections to the superior colliculus in the macaque monkey: a retrograde study using horseradish peroxidase. *J. Comp. Neurol.* 230: 55–76, 1984.

GALLETTI, C. AND BATTAGLINI, P. P. Gaze-dependent visual neurons in area V3a of monkey prestriate cortex. *J. Neurosci.* 9: 1112–1125, 1989.

GOLDBERG, M. E. AND BRUCE, C. J. Primate frontal eye fields. III. Maintenance of a spatially accurate saccade signal. *J. Neurophysiol.* 64: 489–508, 1990.

GUITTON, D., CROMMELINCK, M., AND ROUCOUX, A. Stimulation of the superior colliculus in the alert cat. I. Eye movements and neck EMG activity when the head is restrained. *Exp. Brain Res.* 39: 63–73, 1980.

HARTWICH-YOUNG, R., NELSON, J. S., AND SPARKS, D. L. The perihypoglossal projection to the superior colliculus in the rhesus monkey. *Visual Neurosci.* 4: 29–42, 1990.

HEPP, K., VAN OPSTAL, A. J., STRAUMANN, D., HESS, B. J. M., AND HENN, V. Monkey superior colliculus represents rapid eye movements in a two-dimensional motor map. *J. Neurophysiol.* 69: 965–979, 1993.

HESS, B. J. M. Dual-search coil for measuring 3-dimensional eye movements in experimental animals. *Vision Res.* 30: 597–602, 1990.

HESS, B. J. M., VAN OPSTAL, A. J., STRAUMANN, D., AND HEPP, K. Calibra-

tion of three-dimensional eye position using search coil signals in the rhesus monkey. *Vision Res.* 32: 1647–1654, 1992.

JAY, M. F. AND SPARKS, D. L. Sensorimotor integration in the primate superior colliculus. I. Motor convergence. *J. Neurophysiol.* 57: 22–34, 1987a.

JAY, M. F. AND SPARKS, D. L. Sensorimotor integration in the primate superior colliculus. II. Coordinates of auditory signals. *J. Neurophysiol.* 57: 35–55, 1987b.

JÜRGENS, R., BECKER, W., AND KORNHUBER, H. H. Natural and drug-induced variations of velocity and duration of human saccadic eye movements: evidence for a control of the neural pulse generator by local feedback. *Biol. Cybern.* 39: 87–96, 1981.

KEATING, E. G. AND GOOLEY, S. G. Saccadic disorders caused by cooling the superior colliculus or the frontal eye field, or from combined lesions of both structures. *Brain Res.* 438: 247–255, 1988.

KEATING, E. G., KENNEY, D. V., GOOLEY, S. G., PRATT, S. E., AND MCGILLIS, S. L. Targeting errors and reduced oculomotor range following ablations of the superior colliculus or pretectum/thalamus. *Behav. Brain Res.* 22: 191–210, 1986.

LAL, R. AND FRIEDLANDER, M. J. Effect of passive eye position changes on retinogeniculate transmission in the cat. *J. Neurophysiol.* 63: 502–522, 1990.

LEE, C., ROHRER, W. H., AND SPARKS, D. L. Population coding of saccadic eye movements by neurons in the superior colliculus. *Nature Lond.* 332: 357–360, 1988.

LYNCH, J. C., GRAYBIEL, A. M., AND LOBECK, L. J. The differential projection of two cytoarchiteconic subregions of the inferior parietal lobule of macaque upon the deep layers of the superior colliculus. *J. Comp. Neurol.* 235: 241–254, 1985.

MANLY, B. F. J. *Randomization and Monte Carlo Methods in Biology.* London: Chapman and Hall, 1991.

MAYS, L. E. AND SPARKS, D. L. Dissociation of visual and saccade-related responses in superior colliculus neurons. *J. Neurophysiol.* 43: 207–232, 1980.

MCILWAIN, J. T. Lateral spread of neural excitation during microstimulation in the intermediate gray layer of cat's superior colliculus. *J. Neurophysiol.* 47: 167–178, 1982.

MCILWAIN, J. T. Effects of eye position on saccades evoked electrically from superior colliculus of alert cats. *J. Neurophysiol.* 55: 97–112, 1986.

MCILWAIN, J. T. Topography of eye-position sensitivity of saccades evoked electrically from the cat's superior colliculus. *Visual Neurosci.* 4: 289–298, 1990.

MOORE, R. Y. AND GOLDBERG, J. M. Projections of the inferior colliculus in the monkey. *Exp. Neurol.* 14: 429–438, 1966.

MUNOZ, D. P., PÉLISSON, D., AND GUITTON, D. Movement of neural activity on the superior colliculus motor map during gaze shifts. *Science Wash. DC* 251: 1358–1360, 1991.

MUNOZ, D. P. AND WURTZ, R. H. Fixation cells in monkey superior colliculus. I. Characteristics of cell discharge. *J. Neurophysiol.* 70: 559–575, 1993.

OTTES, F. P., VAN GISBERGEN, J. A. M., AND EGGERMONT, J. J. Visuomotor fields of the superior colliculus: a quantitative model. *Vision Res.* 26: 857–873, 1986.

PECK, C. K. Eye position signals in cat superior colliculus. *Exp. Brain Res.* 61: 447–450, 1986.

PECK, C. K., BARO, J. A., AND WARDER, S. M. Effects of eye position on saccadic eye movements and on the neural responses to auditory and visual stimuli in cat superior colliculus. *Exp. Brain Res.* 103: 227–242, 1995.

PECK, C. K., SCHLAG-REY, M., AND SCHLAG, J. Visuo-oculomotor properties of cells in the superior colliculus of the alert cat. *J. Comp. Neurol.* 194: 97–116, 1980.

PELISSON, D., GUITTON, D., AND MUNOZ, D. P. Compensatory eye and had movements generated by the cat following stimulation-induced perturbations in gaze position. *Exp. Brain Res.* 78: 654–658, 1989.

PRESS, W. H., TEUKOLSKY, S. A., VETTERLING, W. T., AND FLANNERY, B. P. *Numerical Recipes in C* (2nd ed.). Cambridge, UK: Cambridge Univ. Press, 1992.

ROBINSON, D. A. Eye movements evoked by collicular stimulation in the alert monkey. *Vision Res.* 12: 1795–1808, 1972.

ROBINSON, D. A. Oculomotor control signals. In: *Basic Mechanisms of Ocular Motility and Their Clinical Implications,* edited by G. Lennerstrand and P. Bach-y-Rita. New York: Pergamon, 1975, p. 337–374.

ROUCOUX, A. AND CROMMELINCK, M. Eye movements evoked by superior colliculus stimulation in the alert cat. *Brain Res.* 106: 349–363, 1976.

ROUCOUX, A., GUITTON, D., AND CROMMELINCK, M. Stimulation of the superior colliculus of the alert cat. II. Eye and head movements evoked when the head is unrestrained. *Exp. Brain Res.* 39: 75–85, 1980.

SCHILLER, P. H. AND SANDELL, J. H. Interactions between visually and electrically elicited saccades before and after superior colliculus and frontal eye field ablations in the rhesus monkey. *Exp. Brain Res.* 49: 381–392, 1983.

SCHILLER, P. H. AND STRYKER, M. Single-unit recordings and stimulation in superior colliculus of the alert rhesus monkey. *J. Neurophysiol.* 35: 915–924, 1972.

SCUDDER, C. A. A new local feedback model of the saccadic burst generator. *J. Neurophysiol.* 59: 1455–1475, 1988.

SEGRAVES, M. A. AND GOLDBERG, M. E. Initial orbital position affects the trajectories of large saccades evoked by electrical stimulation of the monkey superior colliculus. *Soc. Neurosci. Abstr.* 10, 389, 1984.

SPARKS, D. L. AND MAYS, L. E. Movement fields of saccade-related burst neurons in the monkey superior colliculus. *Brain Res.* 190: 39–50, 1980.

SPARKS, D. L. AND MAYS, L. E. Spatial localization of saccade targets. I. Compensation for stimulation-induced perturbations in eye position. *J. Neurophysiol.* 49: 45–63, 1983.

STANFORD, T. J. AND SPARKS, D. L. Systematic errors for saccades to remembered targets: Evidence for a dissociation between saccade metrics and activity in the superior colliculus. *Vision Res.* 34: 93–106, 1994.

STRYKER, M. P. AND SCHILLER, P. H. Eye and head movements evoked by electrical stimulation of monkey superior colliculus. *Exp. Brain Res.* 23: 103–112, 1975.

TWEED, D. AND VILIS, T. The superior colliculus and spatiotemporal translation in the saccadic system. *Neural Networks* 3: 75–87, 1990.

VAN GISBERGEN, J. A. M., ROBINSON, D. A., AND GIELEN, S. A quantitative analysis of generation of saccadic eye movements by burst neurons. *J. Neurophysiol.* 45: 417–442. 1981.

VAN OPSTAL, A. J. Representation of eye position in three dimensions. In: *Multisensory Control of Movement,* edited by A. Berthoz. Oxford, UK: Oxford Univ. Press, 1993, chapt. 2, p. 27–41.

VAN OPSTAL, A. J. Nonlinearities in the saccadic system and efferent feedback to the collicular motor map. In: *Information Processing Underlying Gaze Control,* edited by J. Delgado-García, P. Vidal, and E. Godeaux. New York: Pergamon, 1994, p. 139–149.

VAN OPSTAL, A. J. AND HEPP, K. A novel interpretation for the collicular role in saccade generation. *Biol. Cybern.* In press.

VAN OPSTAL, A. J., HEPP, K., HESS, B. J. M., STRAUMANN, D., AND HENN, V. Two- rather than three-dimensional representation of saccades in monkey superior colliculus. *Science Wash. DC* 252: 1313–1315, 1991.

VAN OPSTAL, A. J., HEPP, K., HESS, B. J. M., STRAUMANN, D., AND HENN, V. Experimental test of two models for the role of monkey superior colliculus in 3D saccade generation. In: *Multisensory Control of Movement,* edited by A. Berthoz. Oxford, UK: Oxford Univ. Press, 1993, chapt. 16, p. 240–254.

VAN OPSTAL, A. J. AND VAN GISBERGEN, J. A. M. Role of monkey superior colliculus in saccade averaging. *Exp. Brain Res.* 79: 143–149, 1990.

VAN OPSTAL, A. J., VAN GISBERGEN, J. A. M., AND SMIT, A. C. Comparison of saccades evoked by visual stimulation and collicular electrical stimulation in the alert monkey. *Exp. Brain Res.* 79: 299–312, 1990.

WAITZMAN, D. M., MA, T. P., OPTICAN, L. M., AND WURTZ, R. H. Superior colliculus neurons mediate the dynamic characteristics of saccades. *J. Neurophysiol.* 66: 1716–1737, 1991.

WEYAND, T. G. AND MALPELI, J. G. Responses of neurons in primary visual cortex are modulated by eye position. *J. Neurophysiol.* 69: 2258–2260, 1993.

ZIPSER, D. AND ANDERSEN, R. A. A back-propagation programmed network that simulates response properties of a subset of posterior parietal neurons. *Nature Lond.* 331: 679–684, 1988.